SLIDING MODE CONTROL ALGORITHM DEVELOPMENT FOR ANTI-LOCK BRAKE SYSTEM

A THESIS SUBMITTED TO
THE GRADUATE SCHOOL OF NATURAL AND APPLIED SCIENCES
OF
MIDDLE EAST TECHNICAL UNIVERSITY

BY

AHMET OKYAY

IN PARTIAL FULFILLMENT OF THE REQUIREMENTS
FOR
THE DEGREE OF MASTER OF SCIENCE
IN
MECHANICAL ENGINEERING

AUGUST 2011

Approval of the thesis:

SLIDING MODE CONTROL ALGORITHM DEVELOPMENT FOR ANTI-LOCK BRAKE SYSTEM

submitted by **AHMET OKYAY** in partial fulfillment of the requirements of **Master of Science in Mechanical Engineering, Middle East Technical University** by,

Prof. Dr. Canan Özgen _____
Dean, Graduate School of **Natural and Applied Sciences**

Prof. Dr. Suha Oral _____
Head of Department, **Mechanical Engineering**

Assist. Prof. Dr. Ender Ciğeroğlu _____
Supervisor, **Mechanical Engineering Dept., METU**

Assist. Prof. Dr. S. Çağlar Başlamışlı _____
Co-supervisor, **Mechanical Engineering Dept., Hacettepe U.**

Examining Committee Members:

Prof. Dr. M. Kemal Özgören _____
Mechanical Engineering Dept., METU

Assist. Prof. Dr. Ender Ciğeroğlu _____
Mechanical Engineering, Dept., METU

Assist. Prof. Dr. S. Çağlar Başlamışlı _____
Mechanical Engineering Dept., Hacettepe U.

Assist. Prof. Dr. Yiğit Yazıcıoğlu _____
Mechanical Engineering Dept., METU

Assist. Prof. Dr. İlkay Yavrucuk _____
Aerospace Engineering Dept., METU

Date: _____

I hereby declare that all information in this document has been obtained and presented in accordance with academic rules and ethical conduct. I also declare that, as required by these rules and conduct, I have fully cited and referenced all material and results that are not original to this work.

Name, Last Name :

Signature :

ABSTRACT

SLIDING MODE CONTROL ALGORITHM DEVELOPMENT FOR ANTI-LOCK BRAKE SYSTEM

Okyay, Ahmet

M.Sc., Department of Mechanical Engineering

Supervisor : Assist. Prof. Dr. Ender Ciğeroğlu

Co-supervisor : Assist. Prof. Dr. S. Çağlar Başlamışlı

August 2011, 66 pages

In this thesis, a sliding mode controller employing a new sliding surface for antilock brake system (ABS) is proposed, its stability is proven formally and its performance is compared with existing sliding mode controllers. The new sliding mode controller uses the integral-derivative surface, which includes error, its derivative and its integral, all at the same time. This and the already existing derivative surface, which includes error and its derivative only, are named zeroth-order sliding surfaces. Their stability analysis is done using first-order auxiliary surfaces. Auxiliary surfaces equal the sliding surfaces when derivative of the error becomes zero. The first-order error surface, which includes only the error, and the integral surface, which includes error and its integral, were also designed for comparison. During design, tire brake force response is modelled as an uncertainty. Controllers are simulated on a road with an abrupt change in road

coefficient of adhesion. Controller parameters used are optimized, which results in comparable stopping distances while braking on a constant coefficient of adhesion road. Effect of first order actuator dynamics with varying time constants and actuator absolute time delay were considered. Reaching and sliding properties of controllers were also investigated, using results on a constant coefficient of adhesion road. It is observed that zeroth-order sliding surfaces give smoother response for both derivative and integral-derivative cases. As the controllers employing error and derivative surfaces get unstable in the presence of actuator time delay, the integral-derivative surface, proposed in this study, stands as the best controller.

Keywords: Sliding Mode Control, Sliding Surface, Zeroth-Order Sliding Surface, Actuator Time Delay, Auxiliary Surface

ÖZ

KİLİTLENME ÖNLEYİCİ FREN SİSTEMİ (ABS) İÇİN KAYMA KİPİNDE KONTROL ALGORİTMASI GELİŞTİRİLMESİ

Okyay, Ahmet
Yüksek Lisans, Makina Mühendisliği Bölümü
Tez Yöneticisi : Yrd. Doç. Dr. Ender Ciğeroğlu
Ortak Tez Yöneticisi : Yrd. Doç. Dr. S. Çağlar Başlamışlı

Ağustos 2011, 66 sayfa

Bu tezde, kilitlenme önleyici fren sistemi (ABS) için, yeni bir kayma yüzeyi kullanan bir kayma kipinde kontrolcü önerilmiş, kararlılığı matematiksel olarak gösterilmiş ve performansı var olan kayma kipinde kontrolcülerle karşılaştırılmıştır. Yeni kayma kipinde kontrolcü, hatayı, hatanın türevini ve hatanın integralini aynı anda içeren, integral-türev yüzeyini kullanmaktadır. Bu ve zaten var olan, sadece hatayı ve hatanın türevini içeren türev yüzeyi, sıfırıncı-dereceden kayma yüzeyleri olarak adlandırılmıştır. Bu kontrolcülerin kararlılık analizleri birinci dereceden yardımcı yüzeyler kullanılarak yapılmıştır. Hatanın türevi sıfır olduğunda yardımcı yüzeyler kayma yüzeylerine eşittir. Sadece hatayı içeren hata yüzeyi ve hata ile hatanın integralini içeren integral yüzeyi de, karşılaştırma amacıyla tasarlanmıştır. Tasarım sırasında, lastik fren kuvveti cevabı belirsizlik olarak modellenmiştir. Kontrolcüler, sürtünme katsayısında ani bir

değişim bulunan bir yolda benzetime tabi tutulmuştur. Kontrolcü parametreleri, sabit sürtünme katsayısına sahip bir yolda birbirine yakın durma mesafeleri sağlayacak şekilde optimize edilmiştir. Farklı zaman sabitlerine sahip birinci dereceden eyletici dinamikleri ve mutlak eyletici gecikmesinin etkileri hesaba katılmıştır. Sabit sürtünme katsayısına sahip bir yolda, denetçilerin erişme ve kayma özellikleri de araştırılmıştır. Sıfırıncı-dereceden yüzeylerin, hem türev hem de integral-türev durumları için daha pürüzsüz bir cevap verdiği gözlenmiştir. Hata ve türev yüzeylerini kullanan kontrolcüler, eyletici gecikmesi durumunda karasızlaştıkları için, bu çalışmada önerilen sıfırıncı-dereceden integral-türev yüzeyini kullanan kontrolcü, en iyi seçenek olmuştur.

Anahtar Kelimeler: Kayma Kipinde Kontrol, Kayma Yüzeyi, Sıfırıncı-Dereceden Kayma Yüzeyi , Eyletici Gecikmesi,Yardımcı Yüzey

ACKNOWLEDGEMENTS

The author wishes to express his gratitude to his supervisor Assist. Prof. Dr. Ender Ciğeroğlu and co-supervisor Assist. Prof. Dr. S. Çağlar Başlamışlı. Their guidance and encouragement was very important in the development of this work.

The author proudly expresses that he has been a scholar of The National Scholarship Program for M.Sc. Students by The Scientific and Technological Research Council of Turkey (TUBITAK).

TABLE OF CONTENTS

LIST OF FIGURES

LIST OF SYMBOLS

b : input matrix

B_x : stiffness factor

C_x : shape factor

D_x : peak value

e : difference between actual and desired slips.

E_x : curvature factor

f : dynamics of n^{th} – order system

F_x : braking force

F_z : normal force

g : gravitational acceleration

$G_b(s)$: brake torque dynamics

J : moment of inertia of the wheel

K : a positive constant

m : mass of the quarter car

N : ground reaction

p : model parameter for tire model.

q : differential order of error

r : effective radius

S_{Hx} : horizontal shift

S_{Vx} : vertical shift

$\underline{x}$: state vector of n^{th} – order system

$\underline{x}_d$: state reference vector

TB : actuator time constant

T_b : braking torque

u : input

u_{eq} : equivalent control

V : Lyapunov function

V_x : forward velocity

V_s : slip velocity

α : a sliding surface parameter

β : a positive constant

ε : value of average dynamic coefficient of friction

η : a positive controller design parameter

γ : a sliding surface parameter

Γ_b : non-dimensional braking torque

κ : user scaling factor

λ : slip ratio (positive definition)

λ' : slip ratio (negative definition)

λ_d : reference slip ratio

λ_x : shifted slip ratio

μ : dynamic coefficient of friction

$\tilde{\mu}$: uncertain dynamic coefficient of friction

$\bar{\mu}$: average dynamic coefficient of friction

μ_x : tire parameter which affects the maximum braking force

ν : non-dimensional moment of inertia

ω : angular velocity of the wheel

ρ : relay coefficient

σ : sliding surface

σ_0 : zeroth-order sliding surface

τ : actuator time delay constant

CHAPTER I

OVERVIEW OF THE ANTI-LOCK BRAKE SYSTEM

1.1. Necessity of the Anti-Lock Brake System (ABS)

1.1.1. Manual Braking in Emergency Situations

The Anti-Lock Brake System (ABS) has found basis for its development in a number of problems associated with manual braking, especially in emergency conditions. In order to better understand these facts, automobile braking should be redefined in engineering terms.

In a common car, the driver is connected to the brake system via the brake pedal. The brake pedal acts as the interface to the hydraulic brake circuit and allows for the modulation of hydraulic brake pressure. A schematic view of the hydraulic brake system is given in Figure 1. The hydraulic brake pressure determines the braking torque, which acts opposite to the direction of wheel rotation. Although novel systems may have a slightly different outlook, a certain feature of braking is common in all such systems. In all cases, the driver is only capable of controlling the braking torque acting on the wheel, thus affecting wheel deceleration. This is quiet an intriguing fact, as the large inertia of the longitudinally displacing vehicle is independent from wheel rotational inertia. What determines the deceleration of the vehicle body is the longitudinal force formed at the tire-road interface. Therefore, having full control over braking requires substantial knowledge of the complex tire behavior. Brake torque modulation, or wheel deceleration, which is

the sole tool of the driver, only indirectly affects the braking process. Moreover, the driver has a perception of a direct proportionality between the effort applied to the brake pedal and the intensity of braking. This perception quite closely approximates what happens when the brakes are applied for short intervals on a good adhesion road. However, in emergency situations this perception leads to wheel locking and poorer braking forces due to excessive wheel deceleration.

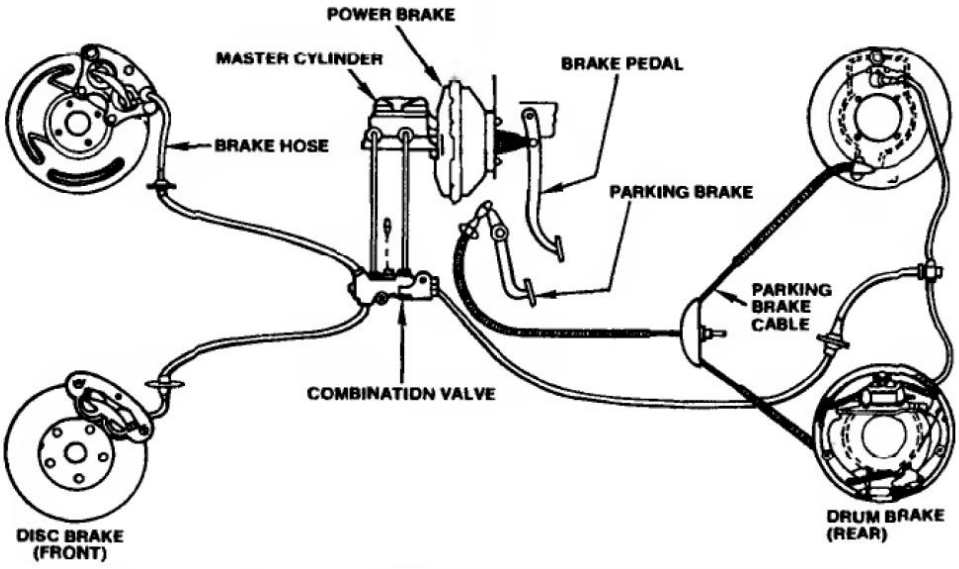

Figure 1. Automobile braking system. (Limpert, 1999)

The primary adversity associated with wheel locking in the case of front wheels, is obviously the loss of directional control due to the lack of lateral forces. In an emergency, this may lead to hazardous accidents as steering away from obstacles or boundaries may be needed together with braking. Furthermore, yaw inputs resulting from split adhesion coefficient roads or effects of side-winds may not be possible to neutralize. In the case of rear wheel locking, vehicle gets unstable. The secondary effect, reduction from the optimum braking force in the case of a locked

wheel, is a less obvious phenomenon. To better understand this and the relation of ABS to traction control, an introduction to tire dynamics and behavior has to be made.

1.1.2. Tire Behavior in Braking

In this section, only some general information will be presented for the sake of clarity. A detailed explanation of tire behavior and model used in this study will be made in subsequent sections. The response of the air filled elastic tire structure is reminiscent of a nonlinear spring; input being the extension of tire outer fibers. However, as the longitudinal forces are formed while the wheel is rotating, a dynamic variable analogous to net displacement is needed. This variable, which was found by experimental evidence to have a governing role in the formation of longitudinal forces, is the *slip ratio.* The *slip ratio,* defined positively for braking, is given by the equation:

$$\lambda = \frac{V_x - r \cdot \omega}{V_x}, \tag{1}$$

where,

V_x: longitudinal speed of car body

r: effective radius

ω: rotational speed of tire.

In the case of a neutral camber angle and absence of side slip (due to steering angle), tire longitudinal force can be written as a function of longitudinal slip ratio and normal force, $F_x = F_z \cdot \mu(\lambda)$. The term $\mu(\lambda)$ refers to the dynamic coefficient of friction.

The importance of slip ratio is a result of its involvement in tire contact patch dynamics. The slip velocity, $V_s = V_x - r\omega$ determines the maximum deformation of tread elements which travel the contact patch (Rajamani, 2006). In free rolling, this quantity is zero. A schematic diagram of the brush model which gives insight in this matter is given in Figure 2. As shown, tread elements can be thought of entering and leaving the contact patch in neutral position, while deformed in between according to the slip velocity. The slip ratio is the scaled version of slip velocity with respect to vehicle longitudinal speed.

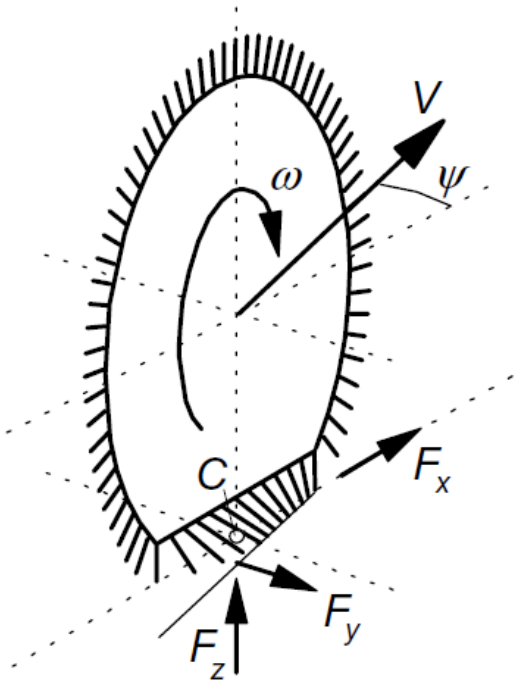

Figure 2. Brush model for tire dynamics; the case for combined longitudinal and lateral slip (Pacejka, 2006).

As observed from Equation (1), tire force is determined by dynamic variables. The driver can directly influence only the rotational speed of wheels. However, the

resulting braking force is determined by the difference between the wheel rotational speed and the car longitudinal speed. Experimental work was done to produce tire force (or dynamic coefficient of friction) curves with respect to the slip ratio. The results were used in the formulation of tire models either by curve fitting or deducing parameters of theoretical models. In each case, the longitudinal brake force coefficient, $\mu = \frac{F_x}{F_z}$, is found to increase almost linearly up to a certain peak and then to decrease quiet abruptly with increasing slip ratio. The initial linear phase is called *stable region* and the latter phase is the *unstable region* (Bosch, 1995). These names are derived according to the fact that keeping the brake torque constant, braking to a point in the stable region produces a constant slip ratio, while eventual wheel locking occurs once it gets into the unstable region (Solyom, 2002). In this study, the Magic Formula Tire Model due to Pacejka, which is a semi-empirical curve fitting method involving an extensive set of shaping and modification factors, is used. The parameter set was taken from the example set given in (Pacejka, 2006). For different road and weather conditions, different sets of tire parameters are needed. On the other hand, there are also less accurate models with less parameters and readily available data for different cases. One of these is the Burckhardt Steady State Tire Model (Burckhardt, 1993). Figure 3 shows the variation of dynamic coefficient of friction for different road and weather conditions, at a longitudinal speed of 25 m/s.

The plots of Figure 3 reveal an important fact we have reserved until now. The wheel locking condition, $\lambda = 1$ produces significantly lower braking forces than at low slip values of about 0.1. Furthermore, there exists a peak slip value which results in highest brake forces. Thus, apart from the prevention of wheel locking, the proper ABS has to track this optimum slip ratio as much as possible.

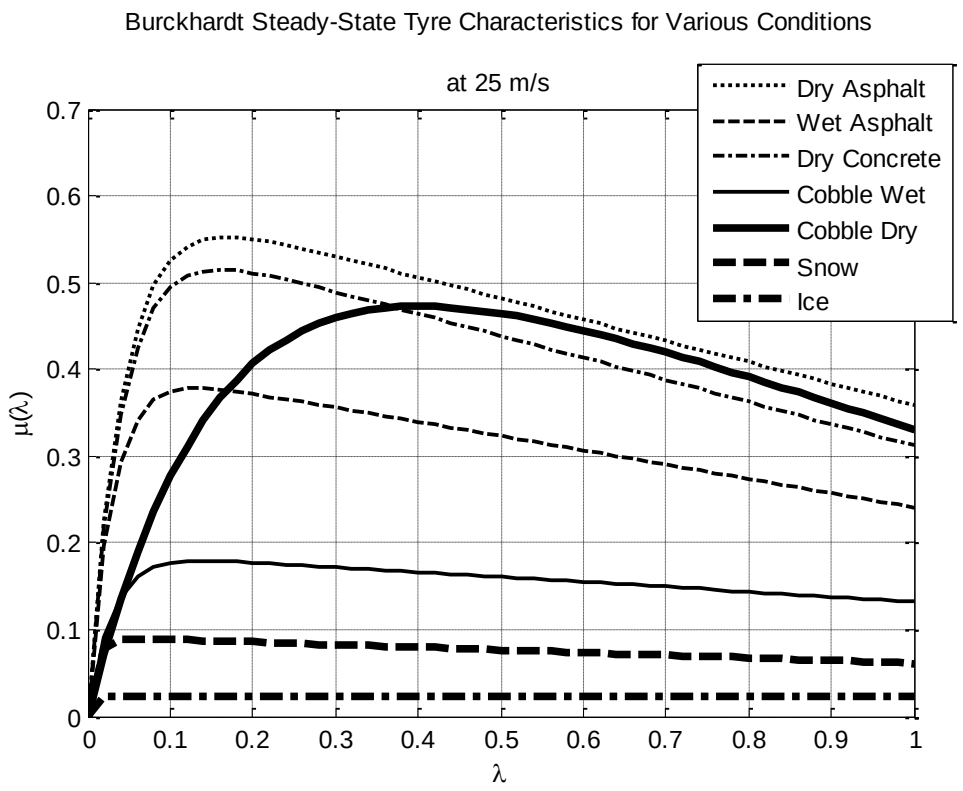

Figure 3. Variation of dynamic coefficient of friction with respect to the slip ratio for varying road and weather conditions, at the speed of 25 m/s.

1.1.3. Aims of the Anti-lock Brake System (ABS)

Until today, numerous industrial and academic studies have been carried out for the development and enhancement of ABS. Each study attempted to improve a certain aspect associated with it. Limpert (1999) and Bosch (1995) give a good outline of those criteria for ABS. The factors which will be handled in this thesis are:

1. ABS must utilize available tire-road friction optimally.
2. ABS must adapt quickly to changes in tire-road friction levels.

Other requirements are about stability, turning, split coefficient of friction, security checks, warnings, steering, etc. The two requirements involved in this thesis are those directly affected by the design methodology of the ABS controller.

1.2. Short History of the Anti-Lock Brake System (ABS)

Skidding has long been a serious problem of wheeled means of transportation. The idea of active braking control systems was studied in the early 1900's for trains. An early patent, "An Improved Safety Device for Preventing the Jamming of the Running Wheels of Automobiles When Braking", dates to 1932. In 1936, a system called "Apparatus for Preventing Wheel Sliding" (US Patent 2038144) due F. B. Thomas was introduced. In the same year, Bosch acquired a similar patent using electromagnetic wheel speed sensors. When wheel locking occurred, an orifice controlled by electric motors regulated brake pressure. In 1940, Fritz Oswald designed and built a non-locking, non-intermittent brake controller. This, like other similar studies, was left unrealized due to their ineffectiveness in reducing stopping distance and providing stability in emergency situations.

Several ABS projects were undertaken in the 1950s. In 1953, Maxaret anti-skid system was developed by Dunlop for aviation industry. Maxaret was a fully mechanical, complex system. In 1972, in England, the Jensen Interceptor automobile became the first production car to offer the Maxaret-based ABS. In 1954, Ford fitted Lincoln sedan with an anti-lock brake system taken from a French aircraft. In 1957, Kelsey-Hayes started their research on automatic braking systems. The problem associated with mechanical systems was that mechanical sensors used were not suitable for working conditions in automobiles and mechanical actuation was too slow to produce notable results.

In the late 1960's and early 1970's, ABS employing analog electronics and vacuum-actuated hydraulic modulation were introduced. In 1968, Kelsey-Hayes

completed the development of a rear-wheel-only ABS. This system was used by Ford in 1969, in Thunderbird and Lincoln Continental Mark III, under the name "Sure Track". In 1971, four-wheel ABS was used in Chrysler Imperial, developed in cooperation with Bendix Corporation. This first four-wheel, three way (two front, one rear) electronically controlled ABS bore the name “Sure Brake”. Also in 1971, GM introduced an electronically controlled rear-wheel-only ABS in Cadillac. ABS was available in GM Eldorado, Toronado, Cadillac Deville and Fleetwood between 1976 and 1982. There were two main weaknesses of these systems. First, system electronics was subject to interferences caused by large working temperature variations, humidity and vibrations. Secondly, slow cycle rates of vacuum actuation significantly increased stopping distances.

Digital electronics were being adapted to ABS in Europe, in the late 1970's. The research on an electronically controlled ABS was already underway in Teldix (affiliate of Telefunken and Bendix Corporation) to put analogue controlled "Tekline" on market. In 1978, Bosch ABS 2, equipping digital technology (instead of analogue) was introduced in Mercedes-Benz S-class cars. In 1980's, ABS improved and found wider application. In 1985, the "integrated" ABS developed by Teves, Mk II, was used in Lincoln Mark VII and Ford Scorpio. This system which integrated servo booster, brake master cylinder and ABS modulator is pictured in Figure 4. It was also the first microprocessor based ABS. In 1986, Kelsey-Hayes introduced the rear-wheel-only ABS for pickup trucks. Delco Moraine NDH began production of its ABS VI system in 1990.

In the model year '91, ABS was offered in approximately one-third of all passenger vehicles, while in 2007, more than three quarters of all new vehicles worldwide were equipped with ABS. (Chrysler, 1970; SAE, 1992; Limpert, 1999; Eckermann, 2001; Garrett, et al., 2001; Savaresi, et. al, 2010).

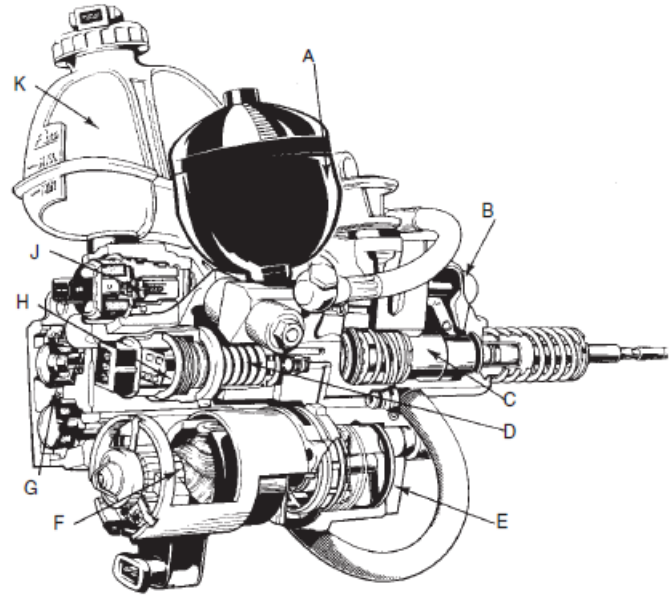

A Hydraulic accumulator
B Control valve
C Hydraulic booster
D ABS master cylinder
E High pressure pump
F Electric moter
G ABS valve block with six solenoid valves
H Pressure warning switch
J Main valve
K Hydraulic fluid reservoir

Figure 4. Teves integrated ABS.

1.3. Conventional Anti-Lock Brake System (ABS)

In the stable range of tire response, from zero slip to the peak braking point, if the braking torque is held in the range of stable braking, an equilibrium slip ratio will be formed (Olson, et al., 2003). Figure 5 shows example of such a response. If there is initially zero slip, slip ratio is going to be attracted to the lower, stable equilibrium.

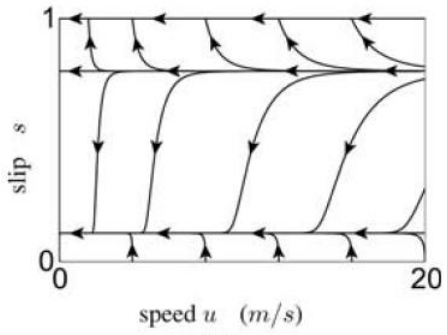

Figure 5. Vehicle dynamic response to a fixed braking torque input. u : car speed, s : slip ratio. (Olson, et al., 2003)

On the stable trajectories of braking (with constant slip), braking force will also remain the same. Thus, wheel deceleration will be determined by the moment differential between the braking torque and the moment of braking force acting on the rim of the wheel. In the stable region, this differential will be rather small (Bosch, 1995). On the other hand, it will increase if the unstable region is entered due to the braking force reduction as presented in Figure 3. Therefore, an abrupt increase in wheel deceleration is expected when instability is initiated. Thus, wheel deceleration can be monitored to deduce stability information. In the widely used Bosch® ABS, these properties of wheel deceleration is employed for ABS control.

The Bosch® ABS is activated whenever tire deceleration exceeds a certain threshold. A typical control cycle for dry road conditions is given in Figure 6. In the figure, $-a$ is the point ABS is switched on.

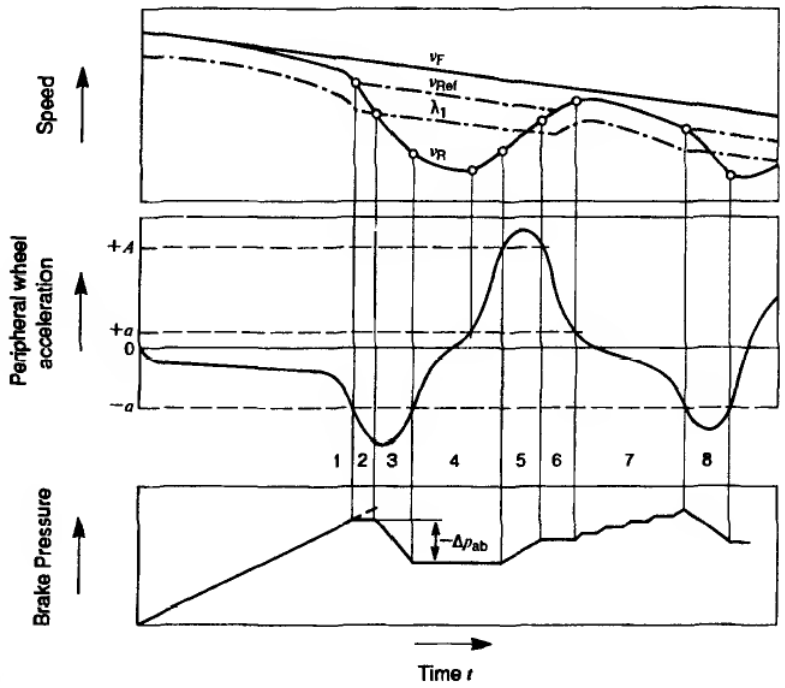

Figure 6. A typical ABS control cycle for dry road conditions. A, a: acceleration/deceleration thresholds, v_F: car speed, v_R: wheel peripheral speed, $v_{\mathrm{Re}f}$: reference speed, λ_1: wheel peripheral speed following reference slip. (Bosch, 1995)

After the ABS is switched on, controller unit forms a reference speed, $v_{\mathrm{Re}f}$ which is the estimated vehicle speed. According to this reference, which is decreasing by a predetermined ramp function, a reference wheel speed, λ_1 is formed. During phase 2, brake pressure is held constant until the slip ratio implied by λ_1 is passed. λ_1 is selected in such a way to prevent under-braking at initial stages, especially on a dry road. In phase 3, brakes switch to the release mode and stay until $-a$ threshold is passed for the second time. Then, a pressure hold mode follows, until $+A$ acceleration limit is reached at the end of phase 4. Phases 5, 6 and 7, activated

by deceleration thresholds, apply and hold brake pressure until $-a$ is reached again. In phase 8, pressure is reduced to let wheel deceleration drop from $-a$. This time, as stopping distance is less affected due to decreased vehicle speed, wheel speed reference is not generated.

Viewing Figure 5, one may be tempted to think that even in the stable region, large wheel decelerations are possible. As increased slip values at constant vehicle speeds correspond to wheel deceleration, the large upward sloping trajectories in stable region (below the lower equilibrium) suggest such a fact. However, in reality, brake torque build-up is a slower process as can be seen in phase 1 of Figure 6. During this process, the lower equilibrium of the phase portrait of Figure 5 is gradually brought upwards by increasing torque. On the other hand, if the critical torque value is exceeded, the lower equilibrium is suddenly vanished. This puts the system on an upwardly sloping trajectory pointed towards the wheel locking condition at $s = 1$. Therefore, keeping brake torque application rate at certain limits, control algorithm can distinguish between decelerations caused by eventual locking and torque application.

The Bosch ABS prevents wheel locking, but optimal braking requires a lot of effort to be put in tuning the equipment. Deceleration thresholds used need to be determined very well and altered according to road conditions, as well as the sequence of brake apply-hold-release phases. The system needs a rich library of instructions for different braking scenarios. Therefore, extensive tests have to be performed to adapt the system to newly designed cars. As a result, this and other rule-based ABS controllers need to be replaced by model based controllers fixing the slip ratio at a predetermined set point.

In this study, the application of sliding-mode controllers to the ABS problem will be investigated. Attention will be focused on the formulation of a better controller, rather than problems associated with realization and instrumentation.

1.4. Anti-lock Brake System (ABS) Control Literature

The emergence of ABS control as a popular academic research topic strongly parallels its historical development in automotive industry. The use of electronics in the late 1960's, boosted opportunities for both manufacturers and academia. Study on an adaptive brake control system by Guntur dates to as early as 1972. Studies at that time were on threshold based logic schemes for constraining the slip within certain bounds during braking. As Guntur has also stated in his thesis (1975), ABS control performed the two main tasks of slip *prediction* and *reselection. Prediction* was the term defining the controller's judgment that the wheel was about to lock. On the other hand, *reselection* involved the reapplication of brakes, considering that the wheel has sufficiently accelerated. The actual slip at the time of prediction was dependent on *initial velocity, rate of application of torque, variables used in prediction* and *threshold values designated for these variables.* Guntur's work was partly involved in obtaining the prediction and reselection methods, which would give the best stopping distance results, while preventing intermittent wheel locking.

In the period 1980-1990, ABS control studies were still in moderate levels. However, controllers with a set-point and error based compensation, rather than logical schemes were emerging. The controller in (Fling and Fenton, 1981) is based on a describing-function approach. Stable, small amplitude limit cycles are secured around the peak slip, using a nonlinear compensator. The work (Tan and Tomizuka, 1990) integrates sliding-mode control with an estimation algorithm for tire/road characteristics. The controller design is taken from a former work dating 1988. The authors of this work have presented their controller in (Tan and Chin, 1991). Being probably the first journal article to present sliding-mode control applied in ABS, their sliding surface comprises both error and derivative of error terms. However, their stability criterion does not guarantee reaching for negative values of switching function. Chin (1992) presents a test validation of the same

controller design. Interestingly, the proposed control law is bang-bang type controller which does not spring from the stability analysis presented. It is known that with a sufficiently large relay term, many sliding-mode controllers can be assured to be stable. Therefore, Chin's is not a strong example, considering rigor. A satisfactory stability analysis for derivative surface was done in (Shim, et al, 2008).

In the 1990's, analytical controller designs for ABS started to capture strong attention from academia. Many of the works in this period have been frequently cited in ABS literature. Controller design approaches employed seem to branch out mainly as fuzzy logic, sliding-mode and neural network controllers.

An extensive survey and general design methodology for fuzzy control systems were given by Lee, C. C. (1990). Fuzzy control was applied to ABS in (Madau, et al., 1993; Layne, et al., 1993; Mauer, 1995). Madau, et al. (1993) tested the efficiency of their rule base on an experimental setup and refined them according to the outcome. Layne, et al. (1993) have applied their *fuzzy model reference learning* algorithm to the ABS control problem. The fuzzy rule base is updated by the algorithm whenever output is significantly deviant from that of the reference model. Mauer (1995) has integrated the fuzzy controller with a discrete logic element for the determination of road conditions, which uses actual slip, brake torque and the results from the slip predictor. Predicted slip is also used in the rule base of fuzzy controller.

The sliding-mode control was also widely studied. Several approaches are presented in (Drakunov, et al., 1995; Kawabe, et al., 1997; Ünsal and Kachroo, 1999; Choi and Cho, 1999; Lee and Sin, 2000). In the paper by Drakunov, et al. (1995), ABS control is achieved by an optimum search for best braking force. Search algorithm is specified in a way that whenever braking force is sufficiently deviant from optimality, trajectories of the system are attracted to a sliding regime

which increases the braking force. Therefore, it is not a sliding-mode controller of the common type. Kawabe, et al. (1997) have designed an integral surface modified for ABS application. They have tested their design in hardware-in-the-loop simulation and on an actual vehicle. Ünsal and Kachroo (1999) have used a nonlinear observer (extended Kalman filter and sliding observers were both considered) for the estimation of difficult to measure car velocity. In the paper by Choi and Cho (1999), a sliding mode controller for actuators employing pulse width modulation is designed and tested on a test bench. Lee and Sin (2000) have also designed a sliding regime using a derivative surface, which is difficult to stabilize. Unfortunately, steps of the stabilization process are not given. Furthermore, their use of the term *equivalent control* is significantly different from Edwards and Spurgeon (1998).

Neural networks were also used in 1990s. Davis, et al. (1992) have designed a neural network controller on a preliminary simulation model with unlimited runs to train the identification and controller networks. Then, they trained them on an *experimental* simulation model with different parameters. Limiting runs on the experimental model to 100, they still obtained promising results.

Although model based and set-point following feedback control systems were increasingly designed in 1990's, the industry still preferred rule based systems. Validation of improvements in the rule base was done by simulations, but this yielded only qualitative data. Wellstead and Pettit's work (1997), employed a then novel piecewise linear analysis method, which allowed for the analysis of the combined nonlinear-dynamic and logic controller systems. The two piecewise linear systems were intermingled to capture dynamic paths of the system. As a result, obscure drawbacks of the initial, intuitive logic controller were discovered and a redesign was made. Yu (1997) have designed a robust adaptive controller for ABS. Bounds of uncertainties are not incorporated directly into the design, but an adaptive law is designed for the dynamics of uncertainty bound estimation.

System is stable in the error domain in terms of both slip error and uncertainty bound estimation error. The controller specified resembles the sliding-mode controller designed with error sliding surface. However, controller dynamics is also governed by a decaying auxiliary signal.

In the period beginning with 2000, ABS control became an area flocked by academicians. Fuzzy control maintained its importance and was used in (Lee and Zak, 2002; Khatun, et al., 2003; Lin and Hsu, 2003a; Precup, et al., 2004; Mirzaei, et al., 2006; Yazicioglu and Unlusoy, 2008; Sahin and Unlusoy, 2010). Lee and Zak (2002) have used genetic algorithms to optimize their fuzzy rule set. Khatun, et al. (2003) have applied fuzzy control to both ABS and traction control, and refined their rule base by experimentation. Lin and Hsu (2003a) have integrated a robust controller with a fuzzy logic controller, where the former compensates for approximation error between the latter and an ideal controller. Precup, et al. (2004) have proposed a Takagi-Sugeno and an interpolative fuzzy controller for ABS. They compared resulting system responses with that of a conventional PI controller. Mirzaei, et al. (2006) have designed a Takagi-Sugeno-Kang type fuzzy controller and optimized both membership functions and rules using genetic algorithms. Yazicioglu and Unlusoy (2008) have designed an ABS for braking performance and steering stability on a nonlinear full car model. Sahin and Unlusoy (2010) have designed a fuzzy logic and a PID controller for ABS for use in integrated active safety systems.

Sliding-mode controllers have also improved after 2000. Notable works in the area include (Schinkel and Hunt, 2002; Wu and Shih, 2003; Lin and Hsu, 2003b; Chun and Sunwoo, 2005; Patel, et al., 2007; Harifi, et al., 2008; Shim, et al., 2008; Amodeo, et al., 2010). Schinkel and Hunt (2002) have started by approximating the nonlinear variation of tire friction coefficient by a piecewise linear relationship. Then, they transformed the whole system to an uncertain piecewise linear system, using operating point linearization for vehicle speed terms. The

resulting system turned out to be unstable for slip values past the peak point. (However, due to the stabilizing effect of the operating point dependent constant input term appearing after linearization, the corresponding system still approaches to the origin.) Then, they designed a sliding-mode like controller, with the equivalent control term slightly changed for reaching the peak slip. For the intermediate region between the two controller structures of different slip bounds, they have designed a PI controller. Wu and Shih (2003) have compared the effects of switching and pulse-width modulation control of hydraulic valves by using the control signal from a sliding-mode controller with derivative surface. However, the formal proof for stability of the controller used is not given. Lin and Hsu (2003b) have used the integral surface in their design. They used a *recurrent neural network (RNN)* to estimate uncertainties. This way, relay coefficient could be reduced, resulting in less chattering. Chun and Sunwoo (2005) have designed a conventional sliding-mode controller with only the error term in sliding surface. Their sole contribution was to feed a higher than necessary reference slip value at the beginning of the braking process, which would decay to its desired level in time. They have neither compared their approach with results of a fixed surface, nor clearly shown the reference slip decay process in simulations. Patel, et al.'s work (2007) is an important example for its rigor and causality. Sliding-mode observers are employed to estimate road/tire characteristics based on a LuGre friction model. Estimated parameters are used in the control law of error surface sliding mode. Furthermore, system is shown to be stable in the sliding-mode, for a given range of parameters. Although stability regarding vehicle velocity is obvious, internal friction variable associated with the tire made analytical proof complicated. Harifi, et al. (2008) have designed an integral surface controller which accounts for uncertainties. Shim, et al. (2008) have investigated the effects of different surface designs on the overall performance of the sliding mode controller. They have given a formal proof to the derivative surface which had been included in many works without being analyzed rigorously. Amodeo, et al. (2010) have designed a second order sliding-mode controller. The difference of

second and higher order modes is that the input term appears in the second derivative (rather than first derivative for first order modes) of the switching function. Therefore, switching effects the derivative of torque, and torque itself becomes continuous. However, chattering free implementation of the algorithm requires correct estimation of many non-measurable states.

Yi, et al. (2002) have proposed an adaptive control algorithm which uses estimated values for optimal slip ratio and overall hydraulic gain. Nouillant, et al. (2002) have designed a fractional controller for ABS. They have also proposed two methods for slip reference generation, namely the *fuzzy logic mapping* and *Pacejka's Inverse Model*.

Recently, Jing, et al. (2011) have designed a switching control strategy for ABS. The advantage of the proposed design is that it is ensured stability within the discontinuous input structure of the industrial ABS. Rather than former designs which necessitate a secondary -though, influential- controller for the tracking of the desired continuous torque by the discontinuous hydraulic brake dynamics, design is constrained by the three ABS modes (brake / hold / release) from the beginning.

CHAPTER II

SLIDING MODE CONTROLLER DESIGN

2.1. Brake System Model

2.1.1. Vehicle and Tire Models

In this study, the quarter car braking model is used to represent braking dynamics of the vehicle, as shown in Figure 7. Values of vehicle parameters are given in Appendix A.1.

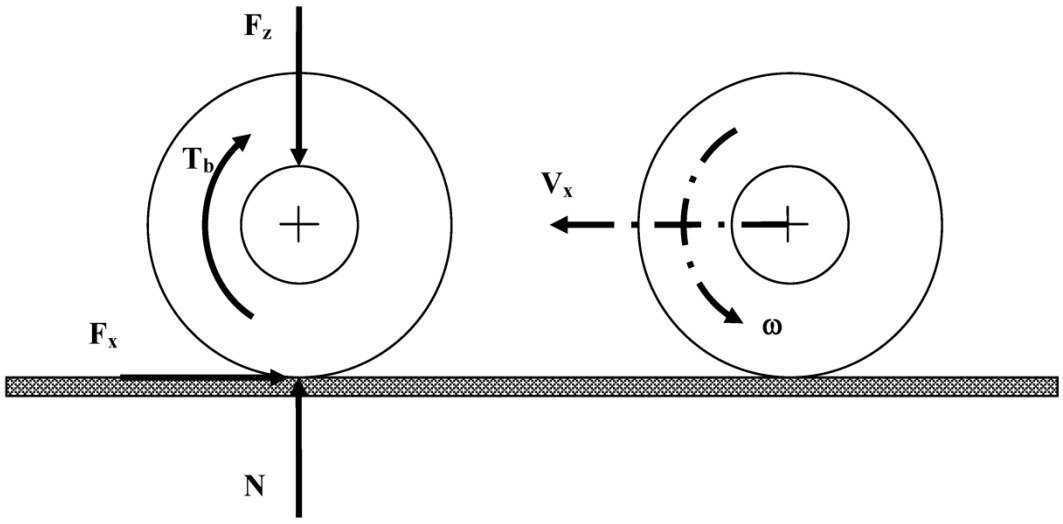

Figure 7. Quarter car model.

Equations of motion for the car model presented are given by,

$$m \cdot \dot{V}_x = -F_x, \tag{2}$$

$$J \cdot \dot{\omega} = r \cdot F_x - T_b, \tag{3}$$

where,

m : mass of the quarter vehicle,

V_x : forward velocity,

F_x : braking force,

J : wheel moment of inertia,

ω : wheel rotational speed,

r : effective radius,

T_b : braking torque.

It is assumed that torque build-up is of first order dynamics. This is a common assumption for electromechanical actuators (Savaresi and Tanelli, 2010). Actuator time constant will be given various values during simulations. Cases with an additional absolute time delay will also be considered. The resulting brake torque dynamics, which results in delays on the brake torque calculated by the controller, can be given as,

$$G_b(s) = \frac{1}{TB \cdot s + 1} \cdot e^{-s \cdot \tau} \tag{4}$$

where,

TB: actuator time constant

τ : actuator time delay constant

The tire model shows the relationship between longitudinal force, F_x and certain other quantities such as car velocity, normal force, slip velocity and slip ratio. The slip ratio is defined as,

$$\lambda' = -\frac{V_s}{V_x}, \tag{5}$$

where the slip velocity, V_s is given by,

$$V_s = V_x - r \cdot \omega . \tag{6}$$

The effective radius, r represents the rolling radius of a freely rolling tire. The Magic Formula Tire Model due to Pacejka (2006), used in this study, is expressed as,

$$F_x = D_x \sin\left[C_x \arctan\left\{ B_x \lambda_x - E_x \left(B_x \lambda_x - \arctan\left(B_x \lambda_x \right) \right) \right\} \right] + S_{Vx}, \tag{7}$$

where

$$\lambda_x = \lambda' + S_{Hx} . \tag{8}$$

The various quantities, $B_x, C_x, D_x, E_x, S_{Vx}$ and S_{Hx} are functions of static tire model parameters p and dynamic variables such as car velocity, slip velocity, slip ratio and normal force. Tire model parameters, p are obtained by special testing procedures. Shaping factors (B_x, C_x, D_x, E_x) and horizontal/vertical shifts $\left(S_{Hx}, S_{Vx}\right)$ can be further modified using "User Scaling Factors", κ, for different

road conditions. Model parameters, scaling factors and equations for shaping factors and shifts are given in the Appendix A.2.

2.1.2. Equations of motion in λ and ω:

For the proper representation and design of the ABS controller, equations of motion given in Equations (2) and (3) are written in terms of slip ratio and forward velocity. In order to simplify the resulting equations, the following non-dimensional parameters are introduced,

$$\nu = \frac{m \cdot r^2}{J}, \tag{9}$$

$$\Gamma_b = \frac{T_b \cdot r}{J \cdot g}. \tag{10}$$

For brevity, Equation (7) is shortened as,

$$F_x = m \cdot g \cdot \mu\left(\lambda, F_z, V_x, \ldots\right) \tag{11}$$

Hence, for braking on a flat road, equations of motion can be obtained as follows:

$$\dot{V}_x = -g \cdot \mu, \tag{12}$$

$$\dot{\lambda} = \frac{g}{V_x}\left[\left(\lambda - 1 - \nu\right) \cdot \mu + \Gamma_b\right], \tag{13}$$

where μ is the dynamic coefficient of friction.

The slip ratio used in (12) and (13) corresponds to the positive definition of slip

ratio for braking, such that,

$$\lambda = \frac{V_s}{V_x}. \tag{14}$$

2.2. Controller Design

The block diagram for the ABS control system is given in Figure 8 below,

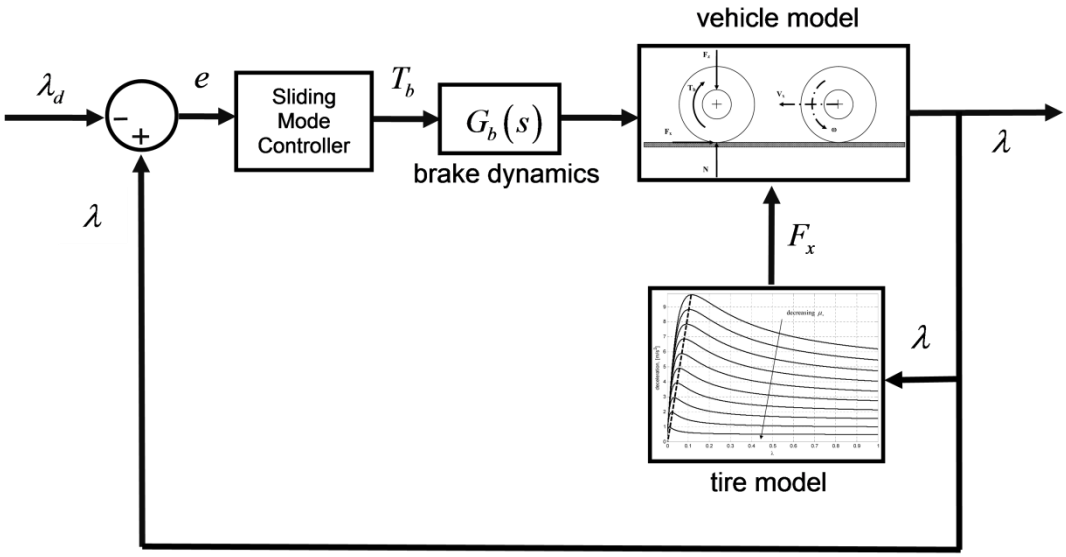

Figure 8. Block diagram for the ABS control system.

By setting the non-dimensional brake torque, Γ_b, as the input to the system, $u = \Gamma_b$, the discontinuous sliding-mode controller using the equivalent control approach is expressed as,

$$u = u_{eq} - \rho \cdot \mathrm{sgn}(\sigma). \tag{15}$$

Extending the simplified notation given by Slotine and Li (1991) to integral control, the sliding surface, $\sigma = 0$, for a general single-input dynamic system of the form $x^{(n)} = f(\underline{x}) + b(\underline{x}) \cdot u$, is given by,

$$\sigma = \left(\frac{d}{dt} + K \right)^{n-1-q} e^{(q)}, \tag{16}$$

$$e = x - x_d, \tag{17}$$

where q takes values from $\{0, -1\}$ and K is strictly positive. $\underline{x}_d = [x_d \quad \dot{x}_d \quad \ddot{x}_d \quad ...]^T$ is the vector of reference states. The case $q = 0$ corresponds to the error surface, while the case $q = -1$ gives the integral surface, i.e. $e^{(-1)} = \int_0^t e \cdot d\tau$. This formulation ensures that discontinuous input term effects the first derivative of sliding surface function, $\dot{\sigma}$. The reachability or the sliding condition for a sliding-mode controller utilizing the form of sliding surface as in Equation (16) is given in (Slotine and Li, 1991), as,

$$\frac{1}{2} \frac{d}{dt} \sigma^2 \leq -\beta |\sigma| \tag{18}$$

To ensure the design of a stabilizing sliding-mode controller, i.e. to constrain system states to approach a sliding surface and stay in the sliding-mode, it is desirable for the sliding surface to be one order lower than the system, as implied by the formulation in Equation (16).

However, exceptions to this can be made at the expense of making a more complicated stability analysis. For example, a certain kind of sliding surfaces can be designated as "derivative" or "zeroth-order" and denoted σ_0. Similar to the definition for sliding surfaces given in Equations (16) and (17), corresponding zeroth-order sliding surfaces can be expressed as,

$$\sigma_0 = \left(\frac{d}{dt} + K \right)^{n-q} e^{(q)}, \tag{19}$$

where K is strictly positive. As their proposed name suggests, they have zero order difference with the system. This property differentiates them from common sliding surfaces. With the inclusion of derivative states, they are no more capable of being stabilized by the simple first-order stabilization strategy employed by the relay part of the sliding-mode controller. The sliding surface itself becomes discontinuous. Therefore, this kind of controllers often needs an auxiliary surface and additional terms in the stability condition.

The form of the reachability condition given in Equation (18) assures finite reaching time. As is common practice, it can also be defined as a Lyapunov stability condition with the Lyapunov function in error domain selected as, $V = \frac{1}{2}\sigma^2$, where $\dot{V} < 0$ is sought for asymptotic stability. Thus, argument of the Lyapunov function determines the final sliding surface. For zeroth-order sliding surfaces, argument of the stability condition may be different from the sliding surface itself, as such surfaces cannot be stabilized in the usual way. Thus, an auxiliary surface, $\sigma^* = 0$, may be used, along with other terms for such cases. For zeroth-order sliding surfaces, the auxiliary surface is obtained from the sliding surface by letting, $\dot{e} \to 0$. By using the auxiliary surface in the stability condition, sliding only on the auxiliary surface is guaranteed, while the actual switching takes place with respect to the sliding surface function, σ.

In the works (Lee and Sin, 2000; Wu and Shih, 2003; Shim, et al., 2008) a "derivative surface" in the form, $\sigma = \dot{e} + \alpha e$ were proposed. In (Lee and Sin, 2000) and (Wu and Shih, 2003), simulations were carried out without giving a formal stability proof. In (Shim, et al., 2008), the stability proof for such a sliding surface used in ABS control was given for the first time. However, the Lyapunov function used was $V = \frac{1}{2} e^2 \, (\sigma^* = e)$, while the sliding surface was $\sigma = \dot{e} + \alpha e$. They have not given account for the difference between the sliding surface and the auxiliary surface used in the stability condition. Stability proof for this controller is given in Section 2.2.2.1 below, within our terms. Furthermore, a new sliding-mode controller is given in Section 2.2.2.2, which utilizes a zeroth-order, integral-derivative sliding surface , $\sigma = \dot{e} + \alpha e + \gamma \int_0^t e \cdot d\tau$, and an auxiliary surface, $\sigma^* = \alpha e + \gamma \int_0^t e \cdot d\tau$.

Apart from the relay part which is directly affected by the sliding surface, the equivalent control, u_{eq}, is also important. This term is the active portion of the control expression, once sliding ($\sigma = 0$) is achieved. In the ideal case, this term ensures staying on the sliding surface by maintaining $\dot{\sigma} = 0$. In such a case, "ideal sliding" occurs. However, this requires that the designer knows all particulars of the system, i.e. there is no uncertainty. In the presence of uncertainties, equivalent control, u_{eq}, will involve uncertain terms. Thus, it is inevitable to omit or average certain variables involved in it. Still, by making equivalent control part close to its ideal version, one needs lower relay coefficients, ρ, to stabilize the system. Hence, intensity of switching is also reduced.

2.2.1. Controllers with First Order Sliding Surfaces

2.2.1.1. Error Surface (Case I)

The error surface with $q = 0$ in Equation (16) is given by,

$$\sigma = e = \lambda - \lambda_d \,, \tag{20}$$

where, λ_d is the desired slip ratio.

The error surface is a limiting case of the sliding-mode controller, as no actual sliding takes place in that case. It arises from the same formulation for actual sliding surfaces when the system is first order.

In our design of the SMC, for all cases, tire response will be considered uncertain. The dynamic coefficient of friction is assumed to be uniformly distributed within known bounds. The uncertain dynamic coefficient of friction, $\tilde{\mu}$, accounts for a number of uncertainties of the system. As seen in Equation (11), it is a function of slip ratio, λ, normal force, F_z, forward velocity, V_x, and a number of other variables which are not effective in our case due to the selection of tire model parameters. Therefore, making controller design for the whole range of this value provides robustness regarding the state of slipping, changes in normal force due to dynamic weight transfer and speed of the vehicle. Controllers of Case I and the three other design cases below, all possess this robustness property. The tire model described in Section 2.1.1 will be used only in simulations. The longitudinal force produced by the uncertain tire model is given as follows,

$$F_x = F_z \cdot \tilde{\mu} \,, \tag{21}$$

where $0 < \tilde{\mu} < 2\varepsilon$ holds. A typical value for ε is 0.5, which will be used in simulations.

Letting $\dot{\sigma} = 0$, the equivalent control is obtained as follows,

$$\frac{g}{V_x}\left[\left(\lambda - 1 - \nu\right)\cdot\tilde{\mu} + \Gamma_b^{eq}\right] - \dot{\lambda}_d = 0. \tag{22}$$

For the uncertain coefficient of friction, $\tilde{\mu}$, the average value can be used as, $\bar{\mu} = \varepsilon$. As the equivalent control is only an approximation due to the presence of uncertainties, $\dot{\lambda}_d$ term can be discarded for simplicity. Stability will be assured by the proper specification of the relay coefficient, ρ. So, the equivalent control can be given as,

$$\Gamma_b^{eq} \triangleq -\varepsilon\cdot\left(\lambda - 1 - \nu\right). \tag{23}$$

For the states designated in the sliding surface to be attracted to the zero error surface, i.e. $\sigma = 0$ achieved, we define a Lyapunov function of the form,

$$V = \frac{1}{2}\sigma^2. \tag{24}$$

Then, stability can be achieved if $\dot{V} = \sigma\dot{\sigma} < 0$ is ensured by the controller. Using the equivalent control in the form of controller given in Equation (15), the condition for stability is given by,

$$\sigma\dot{\sigma} = \sigma\frac{g}{V_x}\left[\left(\lambda - 1 - \nu\right)\cdot\tilde{\mu} - \left(\lambda - 1 - \nu\right)\cdot\bar{\mu} - \rho\,\mathrm{sgn}\left(\sigma\right)\right] - \sigma\dot{\lambda}_d < 0. \tag{25}$$

For the robust design of relay coefficient, ρ, we set up triangle inequality as,

$$\sigma\left[(\lambda-1-\nu)\cdot(\tilde{\mu}-\bar{\mu})\right]-\sigma\frac{V_x}{g}\dot{\lambda}_d<\sigma\cdot\rho\,\mathrm{sgn}(\sigma), \tag{26}$$

$$|\sigma|\cdot\left[|\lambda-1-\nu|\cdot|\tilde{\mu}-\bar{\mu}|\right]+|\sigma|\cdot\frac{V_x}{g}\cdot|\dot{\lambda}_d|<\rho|\sigma|, \tag{27}$$

Using the fact that $|\tilde{\mu}-\bar{\mu}|<\varepsilon$, for robustness,

$$|\sigma|\cdot\left[|\lambda-1-\nu|\cdot\varepsilon\right]+|\sigma|\cdot\frac{V_x}{g}\cdot|\dot{\lambda}_d|<\rho|\sigma|. \tag{28}$$

Cancelling $|\sigma|$'s, one concludes that $\rho>\varepsilon\cdot|\lambda-1-\nu|+\frac{V_x}{g}\cdot|\dot{\lambda}_d|$ is sufficient for robust stability. Then the controller is given by,

$$\Gamma_b=-\varepsilon\cdot(\lambda-1-\nu)-\left(|\lambda-1-\nu|\cdot\varepsilon+\frac{V_x}{g}\cdot|\dot{\lambda}_d|+\eta\right)\cdot\mathrm{sgn}(\sigma), \tag{29}$$

where η is an arbitrary, positive, design quantity.

During the course of controller design, η is usually given an essentially large value. This way, effects of any uncertainties in model parameters and road conditions, which may not be included in controller design, are effectively eliminated. Therefore, in many cases $|\lambda-1-\nu|\cdot\varepsilon$ and $\frac{V_x}{g}\cdot|\dot{\lambda}_d|$ terms can be removed and a single large η can be used as the relay coefficient.

2.2.1.2 Integral Surface (Case II)

This surface corresponds to the integral counterpart of the surface presented in section 2.2.1.1, with $\sigma = e + \gamma \int_0^t e \cdot d\tau$. This time, equivalent control is found as,

$$\dot{\sigma} = \dot{e} + \gamma e = \frac{g}{V_x}\left[(\lambda - 1 - \nu)\cdot\tilde{\mu} + \Gamma_b^{eq}\right] - \dot{\lambda}_d + \gamma e = 0\,, \tag{30}$$

Discarding the $\dot{\lambda}_d$ term as we did in Equation (23),

$$\Gamma_b^{eq} \triangleq -\bar{\mu}\cdot(\lambda - 1 - \nu) - \frac{V_x}{g}\gamma e\,. \tag{31}$$

For stability, defining the Lyapunov function as in Equation (24),

$$\sigma\dot{\sigma} = \sigma\left\{\begin{matrix}\frac{g}{V_x}\left[(\lambda - 1 - \nu)\cdot\tilde{\mu} - (\lambda - 1 - \nu)\cdot\bar{\mu} - \frac{V_x}{g}\gamma e - \rho\,\mathrm{sgn}(\sigma)\right] \\ -\dot{\lambda}_d + \gamma e\end{matrix}\right\} < 0\,, \tag{32}$$

$$\sigma\left\{\frac{g}{V_x}\left[(\lambda - 1 - \nu)\cdot(\tilde{\mu} - \bar{\mu}) - \rho\,\mathrm{sgn}(\sigma)\right]\right\} - \sigma\dot{\lambda}_d < 0\,. \tag{33}$$

We set up the triangle inequality,

$$|\sigma||\lambda - 1 - \nu|\cdot|\tilde{\mu} - \bar{\mu}| + |\sigma|\cdot\frac{V_x}{g}\cdot|\dot{\lambda}_d| < \rho|\sigma|, \tag{34}$$

$$|\sigma||\lambda - 1 - \nu|\cdot\varepsilon + |\sigma|\cdot\frac{V_x}{g}\cdot|\dot{\lambda}_d| < \rho|\sigma|\,. \tag{35}$$

Thus, $\rho = \varepsilon \cdot |\lambda - 1 - \nu| + \frac{V_x}{g} \cdot |\dot{\lambda}_d| + \eta$ achieves robust control. The controller is then given as,

$$\Gamma_b = -\varepsilon \cdot (\lambda - 1 - \nu) - \frac{V_x}{g} \gamma e - \left(\varepsilon \cdot |\lambda - 1 - \nu| + \frac{V_x}{g} \cdot |\dot{\lambda}_d| + \eta \right) \mathrm{sgn}(\sigma). \quad (36)$$

2.2.2. Controllers with Zeroth-Order Sliding Surfaces

2.2.2.1. Derivative Surface (Case III)

This case is the first one of the controllers with zeroth-order sliding surfaces. The zeroth-order sliding surface can be given as,

$$\sigma = \dot{e} + \alpha e, \quad (37)$$

where α is strictly positive.

For the equivalent control, u_{eq}, we set $\sigma = 0$ to stay on the zero error plane. Then,

$$\sigma = \dot{e} + \alpha e = \frac{g}{V_x} \left[(\lambda - 1 - \nu) \cdot \tilde{\mu} + \Gamma_b^{eq} \right] - \dot{\lambda}_d + \alpha e = 0, \quad (38)$$

and

$$\Gamma_b^{eq} \triangleq -(\lambda - 1 - \nu) \cdot \bar{\mu} - \frac{V_x}{g} \alpha e. \quad (39)$$

The equivalent control uses an average value for the uncertain coefficient of friction, $\tilde{\mu}$ and disregards $\dot{\lambda}_d$. This facilitates lowering the magnitude of the relay

part by assisting stability, rather than perfectly following $\sigma = 0$, as in an ideal case.

For the stability of the controller, we use Lyapunov function in the error domain as,

$$V = \frac{1}{2}\left(\sigma^*\right)^2 = \frac{1}{2}e^2, \tag{40}$$

which assures reaching to the auxiliary surface, $\sigma^* = 0$. The auxiliary surface is an exception of the sliding surface, $\sigma = 0$, at $\dot{e} = 0$. Then,

$$\dot{V} = e\dot{e} = \frac{1}{\alpha}\dot{e}\left(\sigma - \dot{e}\right) = \frac{1}{\alpha}\dot{e}\sigma - \frac{1}{\alpha}\dot{e}^2 < 0, \tag{41}$$

should be satisfied. As $-\frac{1}{\alpha}\dot{e}^2$ is ultimately negative, the condition reduces to,

$$\dot{e}\sigma < 0. \tag{42}$$

Then, one may obtain the following relationships consecutively,

$$\sigma \cdot \frac{g}{V_x}\left[\left(\lambda - 1 - \nu\right)\cdot\tilde{\mu} - \left(\lambda - 1 - \nu\right)\cdot\bar{\mu} - \frac{V_x}{g}\alpha e - \rho\,\mathrm{sgn}\left(\sigma\right)\right] - \sigma\dot{\lambda}_d < 0, \tag{43}$$

$$\sigma \cdot \left[\left(\lambda - 1 - \nu\right)\cdot\left(\tilde{\mu} - \bar{\mu}\right) - \frac{V_x}{g}\alpha e\right] - \sigma \cdot \frac{V_x}{g}\cdot\dot{\lambda}_d < \sigma \cdot \rho\,\mathrm{sgn}\left(\sigma\right), \tag{44}$$

$$\sigma \cdot \left[\left(\lambda - 1 - \nu\right)\cdot\left(\tilde{\mu} - \bar{\mu}\right) - \frac{V_x}{g}\alpha e\right] - \sigma \cdot \frac{V_x}{g}\cdot\dot{\lambda}_d < \rho\left|\sigma\right|. \tag{45}$$

Setting the triangle inequality for robustness,

$$|\sigma|\cdot\left[|\lambda-1-\nu|\cdot|\tilde{\mu}-\bar{\mu}|+\frac{V_x}{g}\alpha|e|\right]+|\sigma|\cdot\frac{V_x}{g}\cdot|\dot{\lambda}_d|<\rho|\sigma|, \tag{46}$$

$$|\sigma|\cdot\left[|\lambda-1-\nu|\cdot\varepsilon+\frac{V_x}{g}\alpha|e|\right]+|\sigma|\cdot\frac{V_x}{g}\cdot|\dot{\lambda}_d|<\rho|\sigma|. \tag{47}$$

Finally, the controller is given by,

$$\begin{aligned}\Gamma_b = &-\varepsilon\cdot(\lambda-1-\nu)-\frac{V_x}{g}\alpha e \\ &-\left(\varepsilon\cdot|\lambda-1-\nu|+\frac{V_x}{g}\alpha|e|+\frac{V_x}{g}|\dot{\lambda}_d|+\eta\right)\mathrm{sgn}(\sigma)\end{aligned}. \tag{48}$$

Using the auxiliary surface, $\sigma^*=0$, the controller using the zeroth-order sliding surface, $\sigma=0$ is stabilized for tracking. The resulting controller uses the zeroth-order surface for switching, but is guaranteed only to track $\sigma^*=0$. Effects of this will be investigated in Section 3.

2.2.2.2. Integral-Derivative Surface (Case IV)

In this case, the auxiliary surface, $\sigma^*=\alpha e+\gamma\int_0^t e\cdot d\tau=0$ will be used. The zeroth-order sliding surface is given by,

$$\sigma=\dot{e}+\alpha e+\gamma\int_0^t e\cdot d\tau=0. \tag{49}$$

The equivalent control is found similar to Case III, by setting $\sigma = 0$,

$$\sigma = \dot{e} + \alpha e + \gamma \int_0^t e.d\tau = \frac{g}{V_x}\left[\left(\lambda - 1 - \nu\right)\cdot \tilde{\mu} + \Gamma_b^{eq}\right] - \dot{\lambda}_d + \alpha e + \gamma \int_0^t e.d\tau = 0 \,. \quad (50)$$

Thus,

$$\Gamma_b^{eq} \triangleq -\left(\lambda - 1 - \nu\right)\cdot \bar{\mu} - \frac{V_x}{g}\alpha e - \frac{V_x}{g}\gamma \int_0^t e.d\tau \,. \quad (51)$$

For stability, we define the Lyapunov function in error domain as,

$$V = \frac{1}{2}\left(\sigma^*\right)^2 + \frac{1}{2}\delta e^2, \quad (52)$$

which principally ensures reaching to the auxiliary surface, $\sigma^* = \alpha e + \gamma \int_0^t e \cdot d\tau = 0$.

As for the zeroth-order sliding surface of Case III, this auxiliary surface is also an exception of the sliding surface at $\dot{e} = 0$. The extra term in stability condition, $\frac{1}{2}\delta e^2$, assures that the auxiliary surface, $\sigma^* = 0$ is approached from the correct direction, yielding to the stabilization by switching with respect to σ. Proceeding as in Case III, the following relationships may be consecutively obtained,

$$\dot{V} = \dot{\sigma}^* \sigma^* + \delta \dot{e} e < 0, \quad (53)$$

$$\left(\alpha \dot{e} + \gamma e\right)\left(\alpha e + \gamma \int_0^t e.d\tau\right) + \delta \dot{e} e < 0,$$

$$\alpha^2 \dot{e}e + \alpha\gamma\dot{e}\int_0^t e.d\tau + \alpha\gamma e^2 + \gamma^2 e\int_0^t e.d\tau + \delta\dot{e}e < 0\,,$$

$$\alpha\dot{e}\sigma + \gamma e\sigma - \alpha\dot{e}^2 - \gamma e\dot{e} + \delta\dot{e}e < 0\,. \tag{54}$$

Setting $\delta = \gamma$ and removing the ultimately negative term, the following inequality,

$$\sigma\dot{e} + \frac{\gamma}{\alpha}\sigma e < 0\,, \tag{55}$$

becomes the stability condition. Then,

$$\sigma\left\{\frac{g}{V_x}\left[\left(\lambda - 1 - \nu\right)\cdot\tilde{\mu} + \Gamma_b\right]\right\} - \sigma\dot{\lambda}_d + \frac{\gamma}{\alpha}\sigma e < 0\,, \tag{56}$$

$$\sigma\left\{\frac{g}{V_x}\begin{bmatrix}\left(\lambda - 1 - \nu\right)\cdot\tilde{\mu} - \left(\lambda - 1 - \nu\right)\cdot\bar{\mu} - \dfrac{V_x}{g}\alpha e \\ -\dfrac{V_x}{g}\gamma\displaystyle\int_0^t e.d\tau - \rho\,\mathrm{sgn}\left(\sigma\right)\end{bmatrix}\right\} - \sigma\dot{\lambda}_d + \frac{\gamma}{\alpha}\sigma e < 0\,, \tag{57}$$

$$\begin{aligned}\sigma\left[\left(\lambda - 1 - \nu\right)\cdot\tilde{\mu} - \left(\lambda - 1 - \nu\right)\cdot\bar{\mu} - \frac{V_x}{g}\alpha e - \frac{V_x}{g}\gamma\int_0^t e.d\tau\right] \\ -\sigma\cdot\frac{V_x}{g}\cdot\dot{\lambda}_d + \frac{V_x}{g}\cdot\frac{\gamma}{\alpha}\sigma e < \sigma\rho\,\mathrm{sgn}\left(\sigma\right)\end{aligned}\,. \tag{58}$$

Setting the triangle inequality for robustness,

$$\begin{aligned}|\sigma|\left(\left|\lambda-1-\nu\right|\cdot\left|\tilde{\mu}-\bar{\mu}\right|+\frac{V_x}{g}\alpha|e|+\frac{V_x}{g}\gamma\left|\int_0^t e.d\tau\right|+\frac{V_x}{g}\cdot\frac{\gamma}{\alpha}|e|\right)\\ +|\sigma|\cdot\frac{V_x}{g}\cdot\left|\dot{\lambda}_d\right|<\rho\cdot|\sigma|\end{aligned}, \quad (59)$$

$$\begin{aligned}|\sigma|\left(\varepsilon\cdot\left|\lambda-1-\nu\right|+\frac{V_x}{g}\alpha|e|+\frac{V_x}{g}\gamma\left|\int_0^t e.d\tau\right|+\frac{V_x}{g}\cdot\frac{\gamma}{\alpha}|e|\right)\\ +|\sigma|\cdot\frac{V_x}{g}\cdot\left|\dot{\lambda}_d\right|<\rho\cdot|\sigma|\end{aligned}. \quad (60)$$

The relay coefficient is given by,

$$\rho=\varepsilon\cdot\left|\lambda-1-\nu\right|+\frac{V_x}{g}\left(\alpha+\frac{\gamma}{\alpha}\right)|e|+\frac{V_x}{g}\gamma\left|\int_0^t e.d\tau\right|+\frac{V_x}{g}\cdot\left|\dot{\lambda}_d\right|+\eta\,. \quad (61)$$

Finally, the equation for the controller can be expressed as,

$$\begin{aligned}\Gamma_b=&-\varepsilon\cdot\left(\lambda-1-\nu\right)-\frac{V_x}{g}\alpha e-\frac{V_x}{g}\gamma\int_0^t e.d\tau\\ &-\left(\left|\lambda-1-\nu\right|\cdot\varepsilon+\frac{V_x}{g}\left(\alpha+\frac{\gamma}{\alpha}\right)|e|+\frac{V_x}{g}\gamma\left|\int_0^t e.d\tau\right|+\frac{V_x}{g}\cdot\left|\dot{\lambda}_d\right|+\eta\right)\mathrm{sgn}\left(\sigma\right)\end{aligned} \quad (62)$$

An important property of the controllers in Cases III and IV is that the eventual auxiliary sliding surfaces have the same terms as the actual sliding surfaces of Cases I and II, respectively. Therefore, after the auxiliary surfaces are reached, zeroth-order Cases III and IV track almost first-order surfaces, with additional derivative terms in switching strategy.

2.3. Saturation Function and Reference Forming

Due to the delays/imperfections in actuators and sensors, high frequency oscillations around the sliding surface, known as chattering, is often seen in sliding-mode control. To smoothen these to a certain degree, the saturation function,

$$sat(\sigma) = \begin{cases} \text{sgn}(\sigma), & |\sigma| > \Phi \\ \dfrac{\sigma}{\Phi}, & |\sigma| < \Phi \end{cases}, \tag{63}$$

given in Figure 9 is used, instead of the sign function. In this case, reaching stability is loosened as reaching to the boundary formed by saturation.

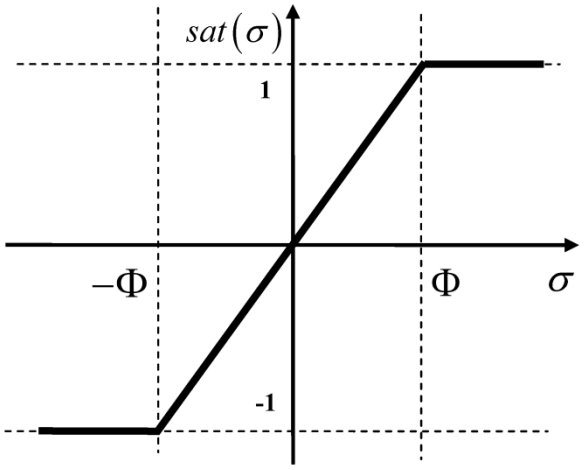

Figure 9. Saturation function.

Another issue in ABS controller design is supplying the reference slip ratio, λ_d, to the controller, which gives the best stopping distance. Various methods are

proposed for this, including the Inverse Pacejka Model used by Nouillant, et al. (2002), used also in (Başlamışlı, et al., 2007). As this study is mainly concerned with exploring the properties of different sliding mode controller structures, this issue is left out for ease in comparison. Optimal reference slip, which gives the lowest stopping distance, will be supplied to the controllers at every instant.

By using the reference slip value, λ_d, which gives the lowest stopping distance, stopping distances can be compared to investigate tracking performance of the controllers. However, in reality, providing such a reference slip is not desirable. Regardless of the extent of utilization of ground adhesion, longitudinal and lateral forces are maximized to the expense of each other. Therefore, having maximal braking forces deteriorates steering response and directional stability in the case of turning while braking. A higher level controller may be necessary to set the reference slip according to the current motion of the vehicle, in the optimal sense. In Section 2.4, controller parameters are optimized for effectively tracking the reference slip, but the formation of the reference slip regarding both varying road conditions and dynamics of the vehicle, are left out.

2.4. Optimization of Controller Parameters

To make an appropriate comparison of controllers, parameters of the sliding-mode controllers designed are optimized using genetic algorithms. Each set of parameters (like a pair of η and γ values for Case II) corresponds to a member with unique genes. Given the bounds of parameter values, the algorithm starts by creating a random population. Members of this population are used as sets of controller design parameters. The cost function, selected as the stopping distance among many other possible alternatives, is evaluated on a straight road with a constant road coefficient of adhesion, $\mu_x = 1.0$. Initial velocity is selected as, $V_x = 30\ m/s$. After the cost function is evaluated for the initial population,

successive populations are created. During their creation, the algorithm either changes (mutates), preserves (considers as elite) or mixes (crossovers) genes of existing members.

During optimization and simulations, saturation function was used with $\Phi = 0.005.$ In reality, much different cases may occur other than the straight road with constant road coefficient of adhesion. However, stability and robustness properties of the designed controllers guarantee controller performance in a wide range of real world emergency braking scenarios, as will be shown in the next section. Optimization results are presented in Table 1 for varying brake actuator time constants, TB.

Table 1. Optimal controller parameters.

Switching Function	TB	η	α	γ	stopping distance [m]
$\sigma = e$	0.20	23.083	-	-	47.82
$\sigma = e$	0.05	51.063	-	-	46.32
$\sigma = e + \gamma \int_0^t e \cdot d\tau$	0.20	25.702	-	0.016	47.82
$\sigma = e + \gamma \int_0^t e \cdot d\tau$	0.05	132.080	-	0.029	46.32
$\sigma = \dot{e} + \alpha e$	0.20	88.065	283.961	-	47.78
$\sigma = \dot{e} + \alpha e$	0.05	79.498	149.277	-	46.31
$\sigma = \dot{e} + \alpha e + \gamma \int_0^t e \cdot d\tau$	0.20	12.145	100.011	1.583	47.77
$\sigma = \dot{e} + \alpha e + \gamma \int_0^t e \cdot d\tau$	0.05	6.104	85.850	7.129	46.31

CHAPTER III

CASE STUDIES

3.1. Reaching and Sliding Results

Before testing the proposed controllers for general operating conditions, their reaching and sliding characteristics are investigated. In this respect, simulations on a constant coefficient of friction road are made with an actuator of time constant, TB=0.05 and without any time delay. For each controller, states making up the sliding surface, $\sigma = 0$, or the auxiliary surface, $\sigma^* = 0$, are plotted in Figure 10. Hence, e is plotted for Cases I and III, while e and $\int_0^t e \cdot d\tau$ are plotted for Cases II and IV.

Comparing Figures 10a-b to 10c-d, it is observed that using the zeroth-order sliding surface has eliminated chattering and oscillations. Both Cases I and III, are stabilized to converge to the state, $e = 0$. With the inclusion of derivative term in sliding surface in Case III, chattering is eliminated (Figure 10c.). Cases II and IV converge to the integral surface, $e + \gamma \int_0^t e \cdot d\tau = 0$. As seen in Figure 10b, oscillations caused by the integrator degrade tracking performance. The improvement of sliding surface in Case IV with the additional derivative term, as seen in Figure 10d, solves this problem.

In Cases III and IV, a zeroth-order sliding surface has been used. Actual switching takes place around $\sigma = 0$, while reaching is guaranteed only to the auxiliary surface, $\sigma^* = 0$, which is first-order. To show how the sliding surface converges to the auxiliary surface, terms of the actual sliding surface are plotted for these cases in Figures 11 and 12.

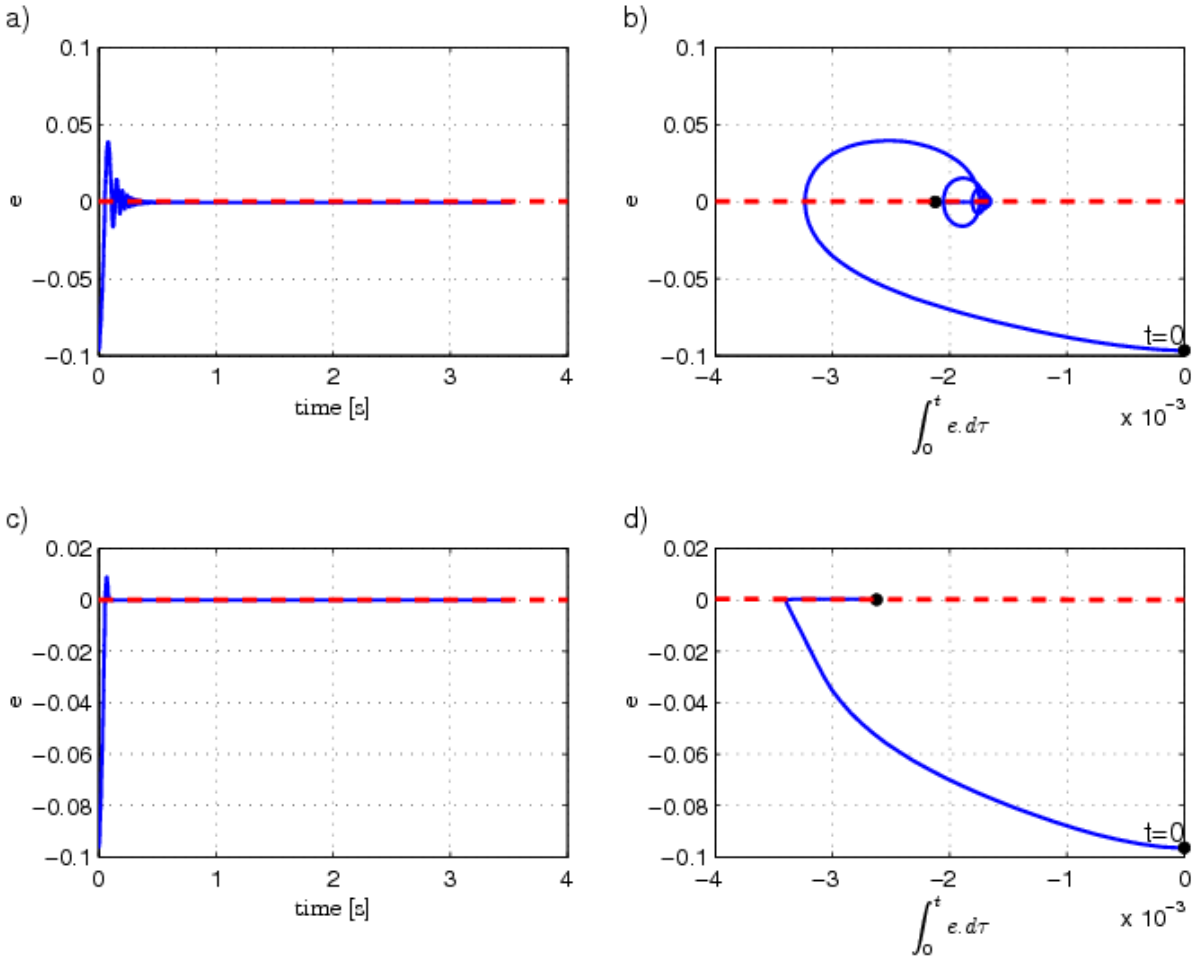

Figure 10. Reaching and sliding properties of controllers. a. Case I, b. Case II, c. Case III, d. Case IV. Final sliding surface is given by the dashed line.

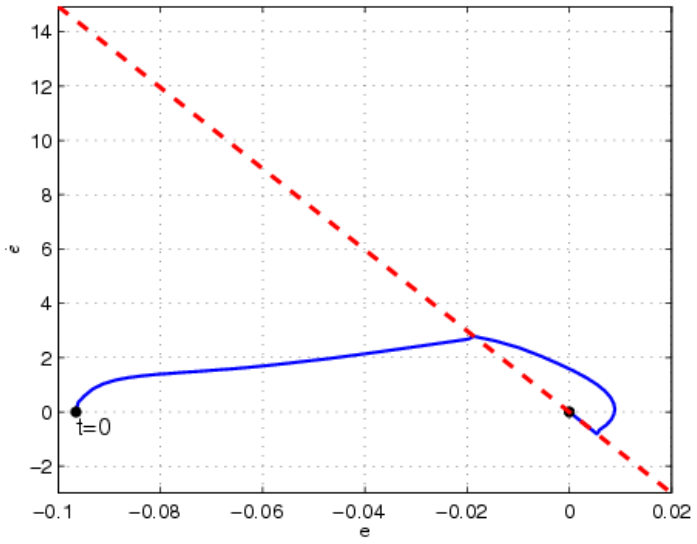

Figure 11. Reaching for Case III. Dashed line represents the sliding surface, $\sigma = 0$.

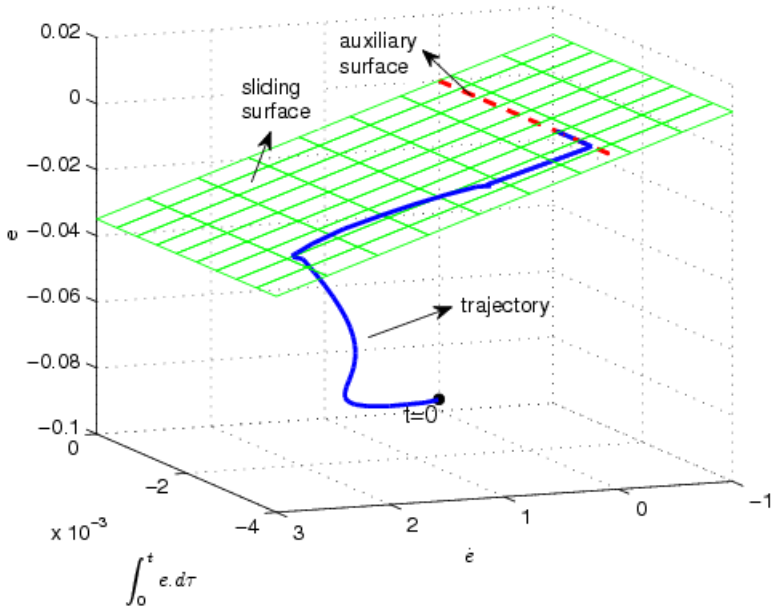

Figure 12. Reaching for Case IV. Green plane represents the sliding surface, $\sigma = 0$. Dashed line is the auxiliary surface, $\sigma^* = 0$.

In both Cases III and IV, it is seen from Figures 11 and 12 that actual switching takes place about the sliding surface, $\sigma = 0$. At $\dot{e} = 0$, the sliding surface and the auxiliary surface become identical. Although the controller of Case III was guaranteed to reach only to the zero error state, $e = 0$, some uncontrived sliding on $\sigma = 0$ also takes place. Similarly, for Case IV, as the system trajectory approaches the auxiliary surface, $\sigma^* = 0$, some sliding on $\sigma = 0$, given by the green plane in Figure 12, takes place. As expected, eventually, the sliding happens on $\sigma^* = 0$.

3.2. Results for Varying Conditions

The more realistic operating conditions of the controllers, simulated in this work, involve sudden changes in road coefficient of friction and time delay in actuators. Among possible changes in road coefficient of friction, the event of suddenly entering a portion of the road with much lower adhesion (like riding over a patch of ice), is very undesirable. In such a case, the moment applied on the wheel hub from the road abruptly drops and if the brake torque is not rapidly decreased, wheel locking occurs. On the other hand, in the case of an actuator time delay, a phase difference between measurement and control manipulation is introduced. This generally has a strongly destabilizing effect. During simulations, the maximum road coefficient of friction, μ_x, is varied such that,

$$\mu_x = \begin{cases} 0.8, & 0 < t \leq 1.5 \\ 0.3, & 1.5 < t < \infty \end{cases}. \tag{64}$$

Actuator time delay is given a typical value as, $\tau = 10\,ms$ (Savaresi and Tanelli, 2010), while time constant of first-order actuator dynamics is varied through cases. The vehicle is braked from an initial speed of $V_x = 30\,m/s$. Results are plotted in Figures 13-20.

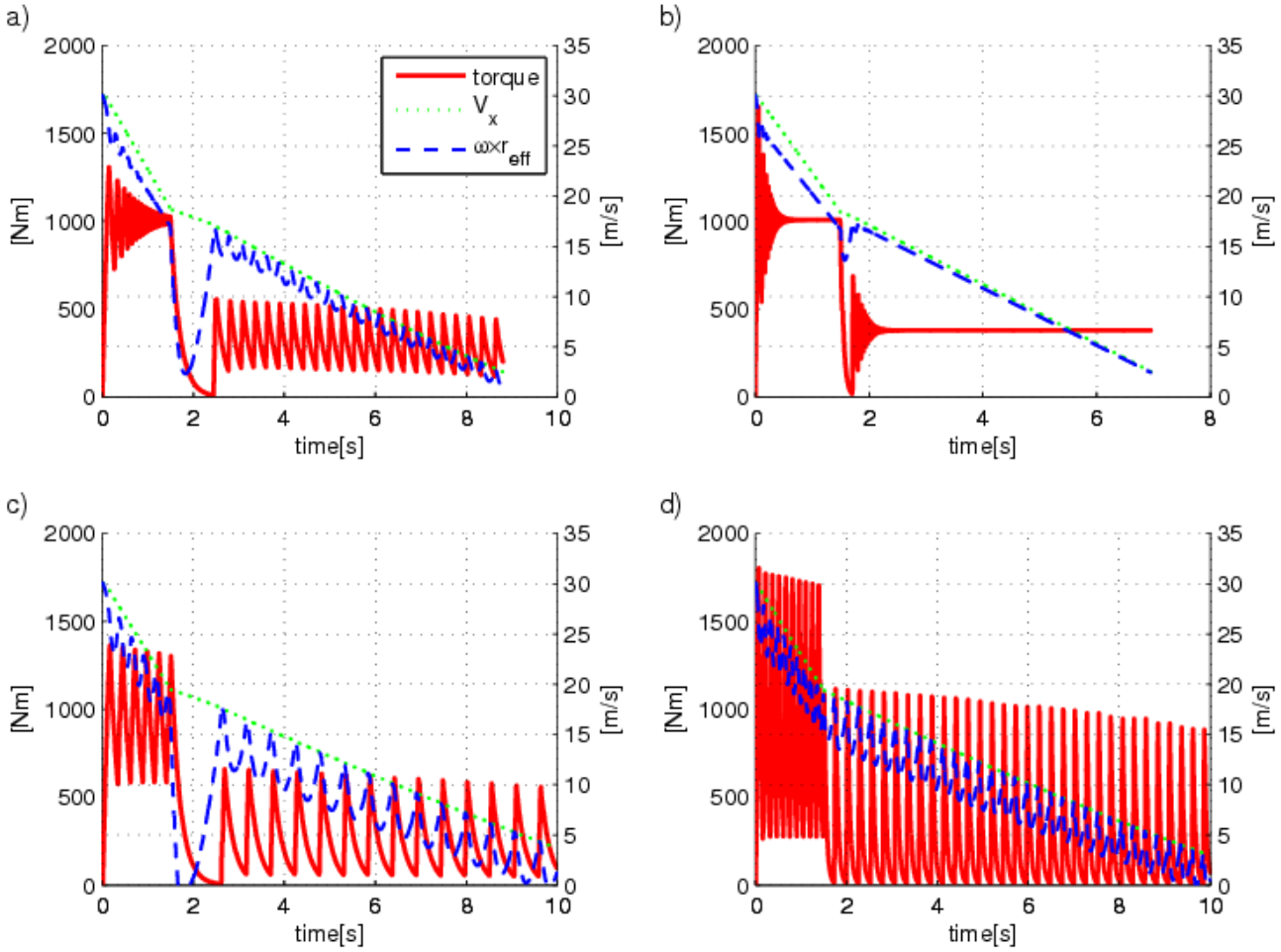

Figure 13. Brake torque, forward velocity and wheel velocity for Case I. a) TB=0.20, b) TB=0.05, c) TB=0.20 with time delay, d) TB=0.05 with time delay.

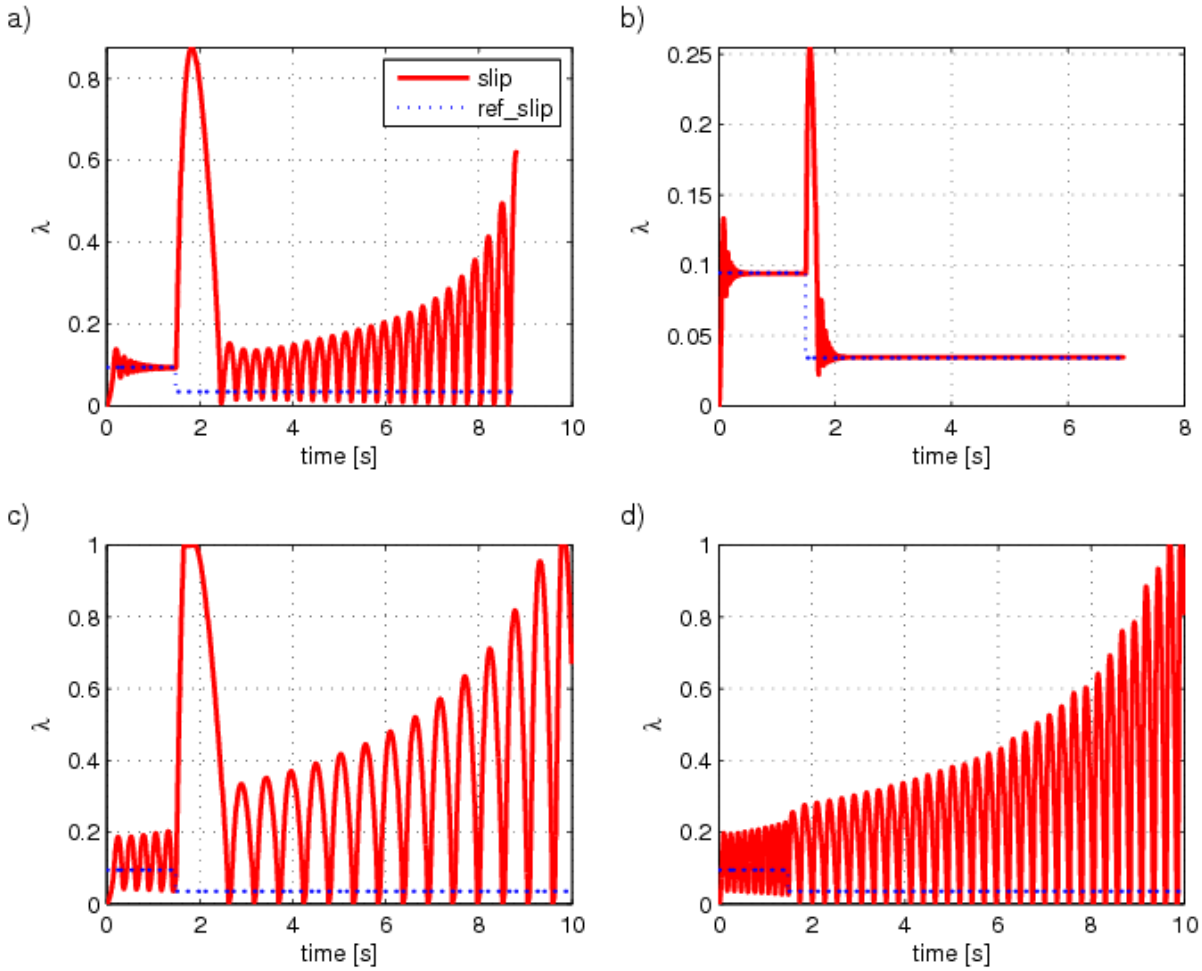

Figure 14. Slip ratio and reference slip ratio for Case I. a) TB=0.20, b) TB=0.05, c) TB=0.20 with time delay, d) TB=0.05 with time delay.

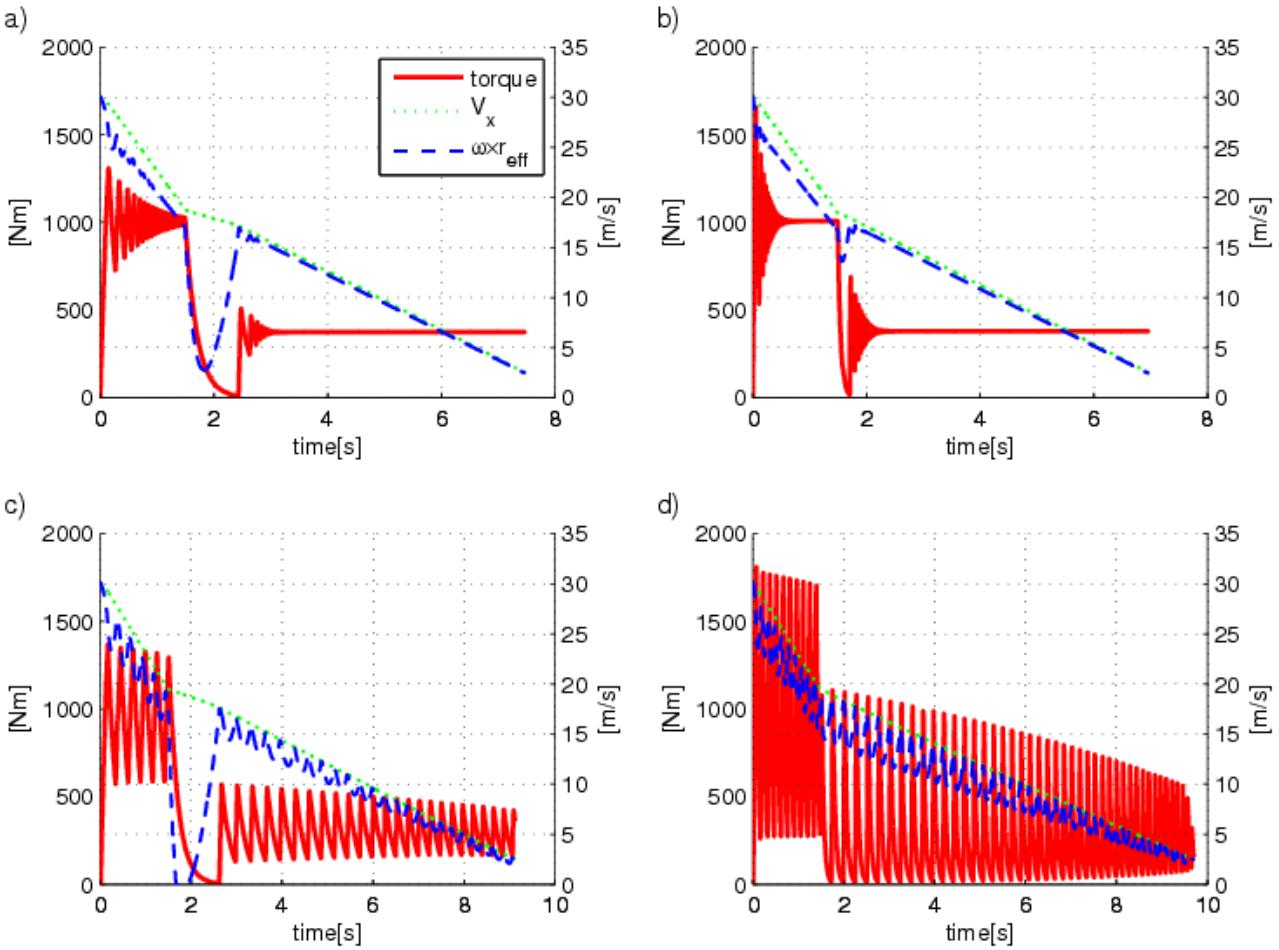

Figure 15. Brake torque, forward velocity and wheel velocity for Case II. a) TB=0.20, b) TB=0.05, c) TB=0.20 with time delay, d) TB=0.05 with time delay.

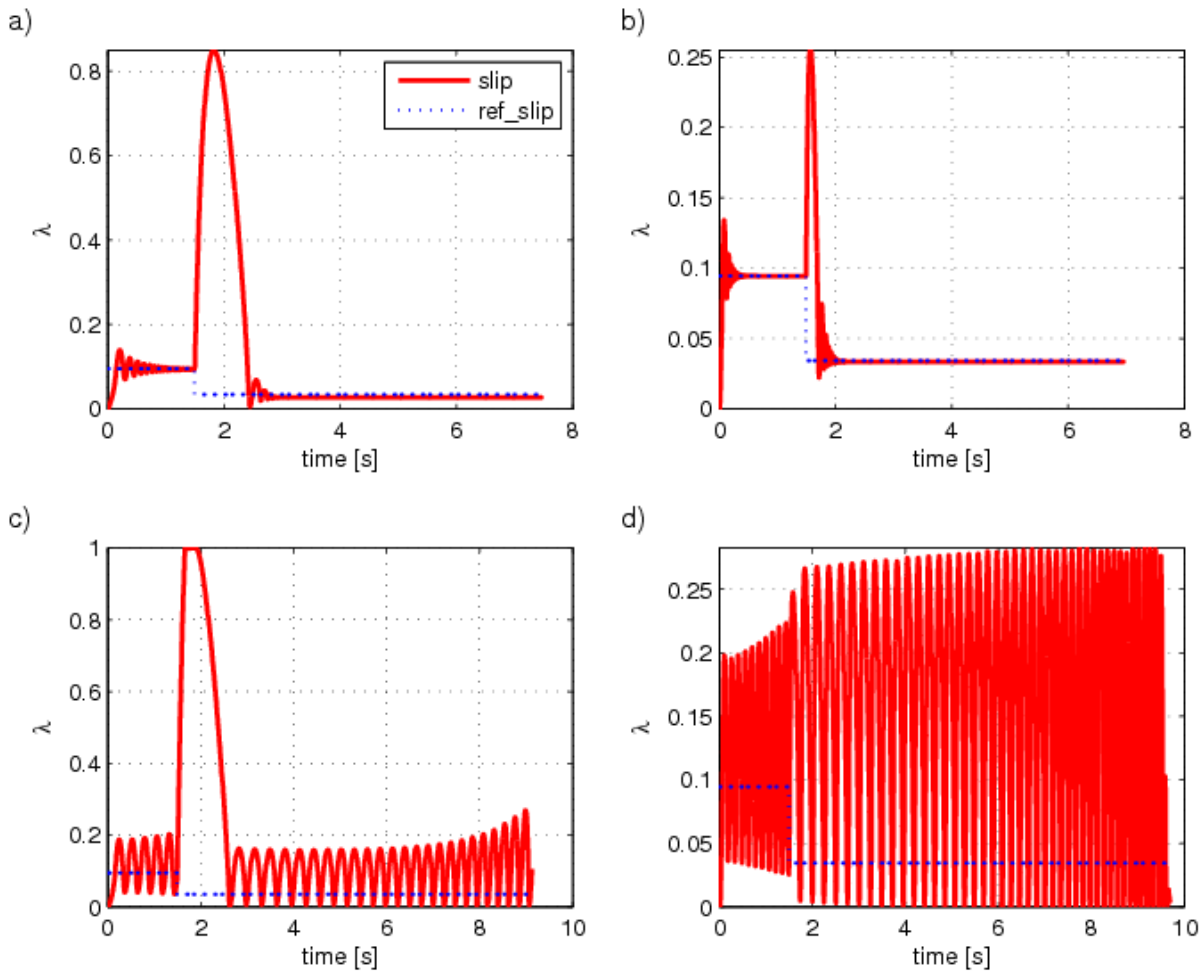

Figure 16. Slip ratio and reference slip ratio for Case II. a) TB=0.20, b) TB=0.05, c) TB=0.20 with time delay, d) TB=0.05 with time delay.

Considering Figures 14b and 16b, with no time delay, tracking performances in the initial phase (until the sudden change of μ_x at $t = 1.5s$) are observed to be similar for the fast actuator, TB=0.05. On the other hand, for TB=0.20, oscillations about the reference slip tend to increase for Case I (Figure 14a). This adversity of the slow actuator is eliminated in Case II (Figure 16a). Therefore, the integral surface is robust to instability caused by actuator first-order delays.

At $t = 1.5s$, an abrupt change in road coefficient of friction is introduced. This change causes a sharp rise in slip ratio, especially in cases when the actuator cannot react in time, as in seen in Figures 14a and 16a, compared to Figures 14b and 16b.

In the cases involving actuator time delay, the error surface (Case I) is observed to get unstable with increasing magnitude of oscillations (Figures 14c-d). It is interesting that increased actuator speed only worsens the situation by increasing frequency. On the other hand, as seen from Figures 16c and 16d, the integral surface (Case II) remains stable. Therefore, the integral surface is robust to actuator time delays.

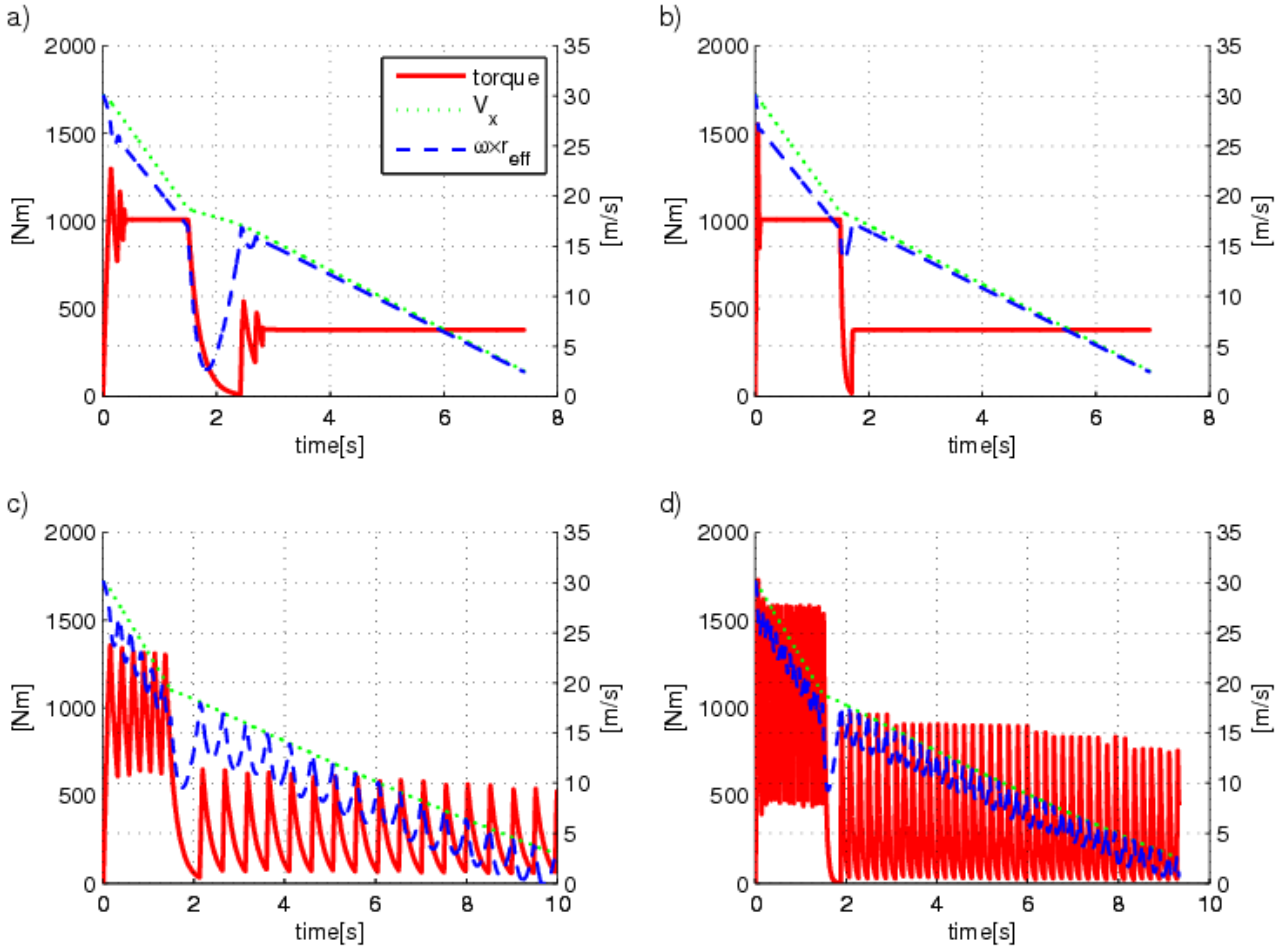

Figure 17. Brake torque, forward velocity and wheel velocity for Case III. a) TB=0.20, b) TB=0.05, c) TB=0.20 with time delay, d) TB=0.05 with time delay.

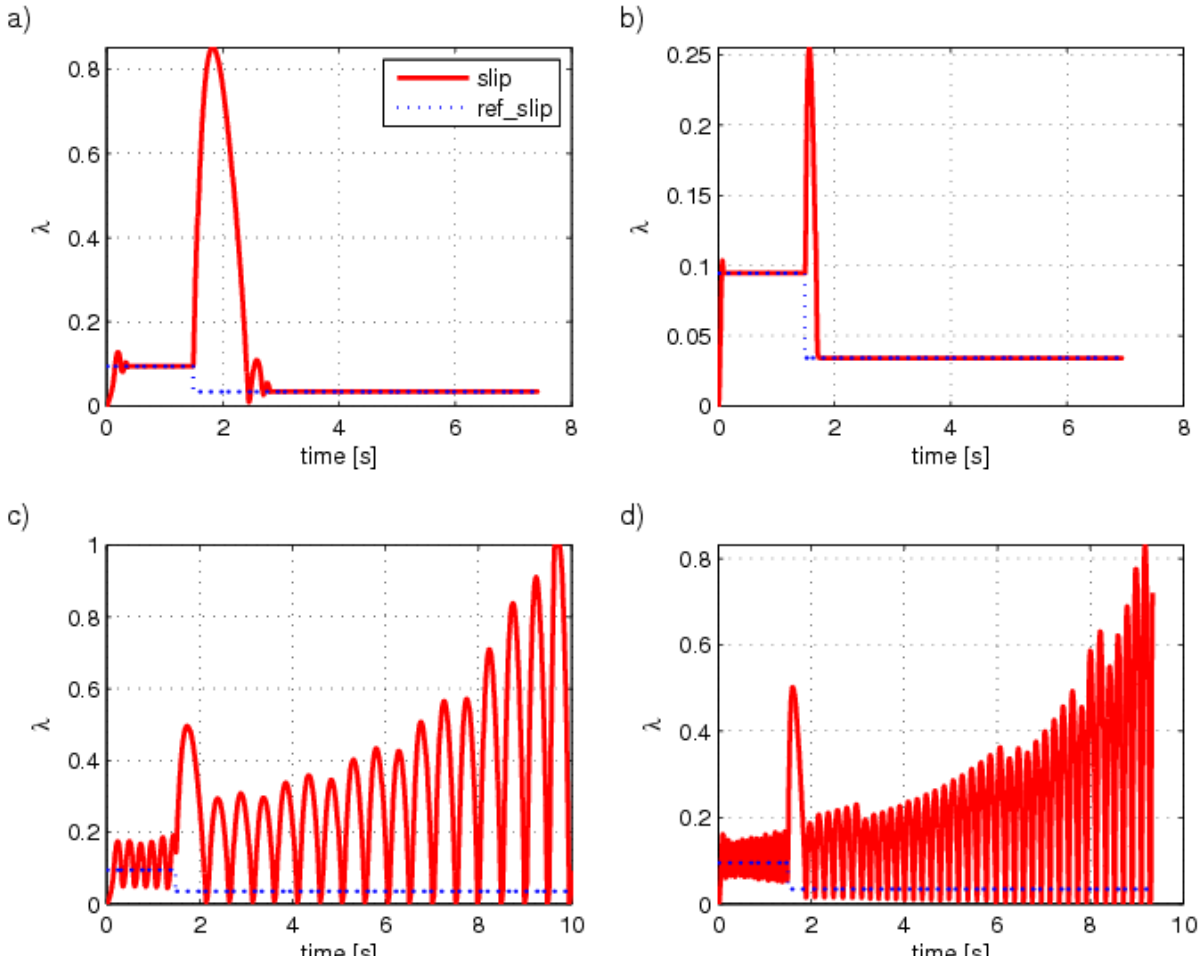

Figure 18. Slip ratio and reference slip ratio for Case III. a) TB=0.20, b) TB=0.05, c) TB=0.20 with time delay, d) TB=0.05 with time delay.

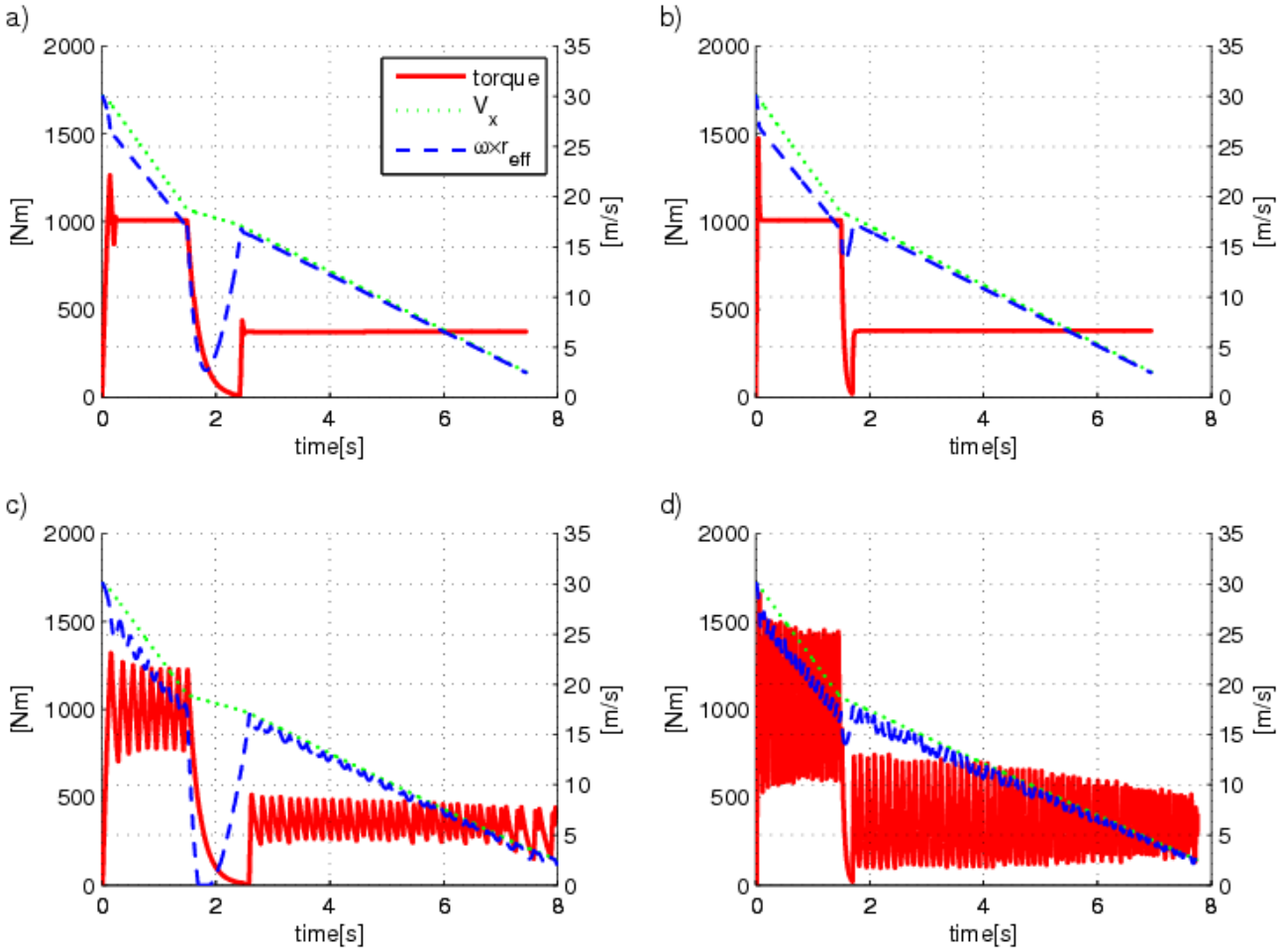

Figure 19. Brake torque, forward velocity and wheel velocity for Case IV. a) TB=0.20, b) TB=0.05, c) TB=0.20 with time delay, d) TB=0.05 with time delay.

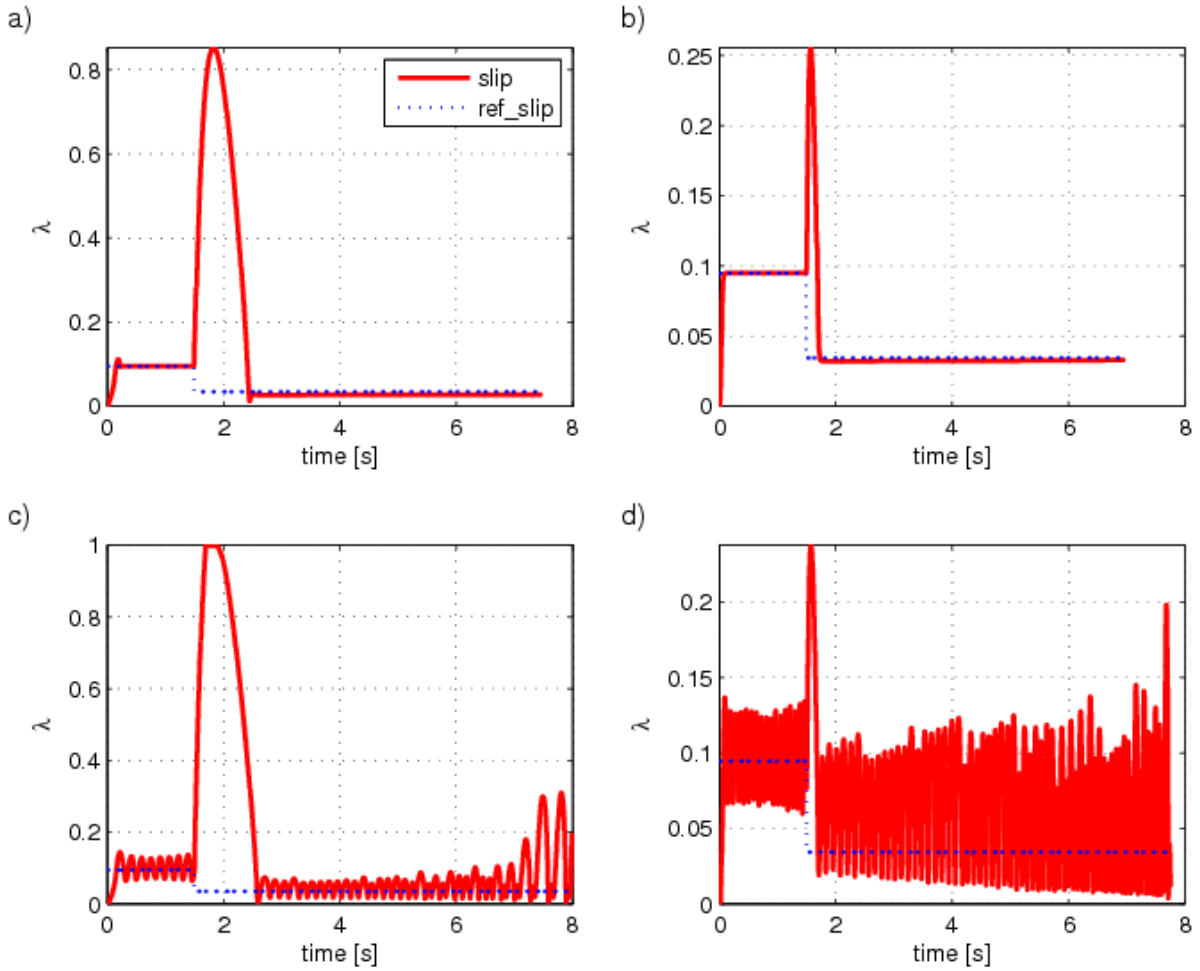

Figure 20. Slip ratio and reference slip ratio for Case IV. a) TB=0.20, b) TB=0.05, c) TB=0.20 with time delay, d) TB=0.05 with time delay.

From Figures 17a-b and 19a-b the effect of using derivative term in sliding surface can be observed. Comparing Figures 17a-b (Case III) to 13a-b (Case I), it is seen that chattering has almost vanished for the derivative surface. A similar situation is present for the integral-derivative surface (Cases IV-II), as observed from Figures 19a-b and 15a-b. In Case III, instability caused by slow actuation, has also been eliminated by using the derivative term (Figures 14a and 18a).

In both Cases III and IV, excellent tracking is observed in the absence of time delay (Figures 18a-b and 20a-b). However, in the case of actuator time delay, Figures 18c-d reveal that change of the switching strategy from Case I to III, could not prevent instability for the resulting error surface. On the other hand, in the case of integral-derivative surface, in Case IV, stability is preserved with smaller oscillations compared to Case II (Figure 16c-d and 20c-d).

CHAPTER IV

CONCLUSIONS

In this study, performances of sliding-mode controllers employing different sliding surfaces of different order are compared for ABS slip control. In all cases, tire behavior is considered as an uncertainty and controllers are stabilized for the whole range of resulting dynamic coefficients of friction.

In Cases I and II, common sliding surface designs are used, for which reaching the sliding surface can be assured by the stability analysis involving only the sliding surface. On the other hand, Cases III and IV involve zeroth-order sliding surfaces, stability of which cannot be assured by the bang-bang strategy of the sliding-mode controller. For these cases, stability condition is constructed for auxiliary surfaces which are sub-surfaces or exceptions of the sliding surface. Although the eventual auxiliary sliding surfaces of Cases III and IV are the same as the actual sliding surfaces of Cases I and II, the modification introduced substantially affects controller behavior.

It is seen that having the derivative of the error in the sliding surface and stabilizing the controller with this strategy reduces chattering and improves tracking for both derivative and integral-derivative surfaces (Cases III and IV). These cases achieve sliding on the auxiliary, first-order surfaces more smoothly. Although they were stabilized only for the auxiliary surface, while reaching it, some sliding also takes place on the zeroth-order sliding surface.

Investigating performances in the face of actuator time delay, error and derivative surfaces are seen to get unstable, while the integral and integral-derivative surfaces perform well. Therefore, sliding on the integral surface, either with an integral switching strategy or as the eventual result of the zeroth-order integral-derivative switching strategy, is robust to actuator time delays. As a result, the zeroth-order integral-derivative surface (Case IV), stabilized for the auxiliary first-order sliding surface, proposed in this study, stands as the best option.

During controller design, it was assumed that slip values could be measured. However, in reality, observers could be necessary, as direct measurement devices may be unavailable. Furthermore, observers could still be used in order to decrease processing times. As a future study, performance of the controllers coupled with slip observers can be investigated. Observer designs can be made using sliding-mode control theory. Furthermore, new observer designs can be made employing zeroth-order sliding surfaces.

REFERENCES

Amodeo, M., Ferrara, A., Terzaghi, R. and Vecchio, C. (2010). *Wheel slip control via second-order sliding-mode generation.* IEEE T. Intell. Transp., 11(1), pp. 122-131.

Başlamışlı, S. Ç., Köse, İ. E. and Anlaş, G. (2007). *Robust control of antilock brake system*. Vehicle Syst. Dyn. 45(3), pp. 217-232.

Bosch (1995). Automotive Brake Systems, Stuttgart: Robert Bosch GmbH.

Burckhardt, M. (1993). Fahrwerktechnik: Radschlupfregelsysteme, Germany: Vogel-Verlag.

Choi, S. and Cho, D.-W. (1999). *Control of wheel slip ratio using sliding mode controller with pulse width modulator.* Vehicle Syst. Dyn. 32(4,5), pp. 267-284.

Chrysler Motors Corporation (1970). Press Release: Four Wheel Sure Brake. *available from*: http://www.imperialclub.com/Yr/1971/SureBrake/ (last accessed on 07.05.2011)

Chun, K. and Sunwoo, M. (2005). *Wheel slip tracking using moving sliding surface.* P. I. Mech. Eng. D.-J. Aut., 219(1), pp. 31-41.

Davis, L. I., Puskorius, G. V., Yuan, F. and Feldkamp, L. A. (1992). *Neural network modeling and control of an anti-lock brake system.* In Proc., Intelligent Vehicles '92 Symp., 29 Jun - 1 Jul 1992, Detroit, MI, USA, pp. 179-184.

Drakunov, S., Ozguner, U., Dix, P. and Ashrafi, B. (1995). *ABS control using optimum search via sliding modes*. IEEE T. Contr. Syst. T., 3(1), pp. 79-85.

Eckermann, E. (2001). World History of the Automobile. Warrendale, PA: SAE.

Edwards, C. and Spurgeon, S. K. (1998). Sliding Mode Control: Theory and Applications, UK: Taylor & Francis.

Fling, R. T. and Fenton, R. E. (1981). *A describing-function approach to anti-skid design.* IEEE T. Veh. Technol., 30(3), pp. 134-144.

Fridman, L., Levant, A. (2002). Chapter 3: Higher order sliding modes. In: Perruquetti, W. and Barbot, J. P., Eds. Sliding Mode Control in Engineering, New York: Marcel Dekker, pp. 70-118.

Garrett, T. K., Newton, K. and Steeds, W. (2001). The Motor Vehicle, 13th Edition, UK: Butterworth-Heinemann.

Guntur, R. R. (1975). *Adaptive brake control systems: Some considerations on design, development and evaluation of rear wheel brake control systems.* Ph.D. Dissertation, TU Delft.

Guntur, R. R. and Ouwerkerk, H (1972). *Adaptive brake control system*. P. I. Mech. Eng. D.-J. Aut., 186, pp. 855-880.

Harifi, A., Aghagolzadeh, A., Alizadeh, G. and Sadeghi, M. (2008). *Designing a sliding mode controller for slip control of antilock brake systems*. Transport. Res. C.- Emer., 16(6), pp. 731-741.

Jing, H., Liu, Z. and Chen, H. (2011). *A switched control strategy for antilock braking system with on/off valves.* IEEE T. Veh. Technol., 60(4), pp. 1470-1484.

Johansen, T. A., Petersen, I., Kalkkuhl, J. and Lüdemann, J. (2003). *Gain-scheduled wheel slip control in automotive brake systems*. IEEE T. Contr. Syst. T., 11(6), pp. 799-811.

Kawabe, T., Nakazawa, M., Notsu, I. and Watanabe, Y. (1997). *A sliding mode controller for wheel slip ratio control system.* Vehicle Syst. Dyn., 27(5-6), pp. 393-408.

Khatun, P., Bingham C. M., Schofield, N. and Mellor, P. H. (2003). *Application of fuzzy control algorithms for electric vehicle antilock braking/traction control systems.* IEEE T. Veh. Technol., 52(5), pp. 1356-1364.

Layne, J. R., Passino, K. M. and Yurkovich, S. (1993). *Fuzzy learning control for antiskid braking systems.* IEEE T. Contr. Syst. T., 1(2), pp. 122-129.

Lee, B.-R. and Sin, K.-H. (2000). *Slip-ratio control of ABS using sliding mode control.* In Proc., The 4th Korea-Russia Int. Symp. Science and Technology, 2000, KORUS 2000, 27 Jun - 01 Jul 2000, Ulsan, South Korea, vol. 3, pp. 72-77.

Lee, C. C. (1990). *Fuzzy logic in control systems: Fuzzy logic controller- Part I, II.* IEEE T. Syst. Man Cy., 20(2), pp. 404-435.

Lee, Y. and Zak, H. S. (2002). *Designing a genetic neural fuzzy antilock-brake-system controller.* IEEE T. Evolut. Comput., 6(2), pp. 198-211.

Limpert, R. (1999). Brake Design and Safety, 2nd Edition, Warrendale, Pa: SAE.

Lin, C. and Hsu, C. (2003a). *Self-learning fuzzy sliding-mode control for antilock braking systems*. IEEE T. Contr. Syst. Technol., 11(2), pp. 273-278.

Lin, C. and Hsu, C. (2003b). *Neural-network hybrid control for antilock braking systems*. IEEE T. Neural Networ., 14(2), pp. 351-359.

Madau, D. P., Yuan, F., Davis, Jr., L. I. and Feldkamp, L. A. (1993). *Fuzzy logic anti-lock brake system for a limited range coefficient of friction surface.* In Proc., Second IEEE Int. Conf. Fuzzy Systems, 28 Mar - 1 Apr 1993, San Francisco, CA, USA, vol. 2, pp. 883-888.

Mauer, G. F. (1995). *A fuzzy logic controller for an ABS braking system.* IEEE T. Fuzzy Syst., 3(4), pp. 381-388.

Mirzaei, A., Moallem, M., Dehkordi, B. M. and Fahimi, B. (2006). *Design of an optimal fuzzy controller for antilock braking systems.* IEEE T. Veh. Technol., 55(6), pp. 1725-1730.

Mirzaeinejad, H. and Mirzaei, M. (2010). *A novel method for non-linear control of wheel slip in anti-lock braking systems*. Control Eng. Pract., 18(8), pp. 918–926.

Nouillant, C., Assadian, F., Moreau, X. and Oustaloup, A. (2002). *Feedforward and CRONE feedback control strategies for automobile ABS*. Vehicle Syst. Dyn., 38(4), pp. 293- 315.

Olson, B. J. , Shaw, S. W. and Stépán, G. (2003). *Nonlinear dynamics of vehicle traction*, Vehicle Syst. Dyn., 40(6), pp. 377-399.

Pacejka, H. B. (2006). Tire and Vehicle Dynamics, 2nd Edition, Oxford: Butterworth-Heinemann.

Patel, N., Edwards, C. and Spurgeon, S. K. (2007). *Optimal braking and estimation of tyre friction in automotive vehicles using sliding modes.* Int. J. Syst. Sci., 38(11), pp. 901-912.

Precup, R. E., Preitl, S., Balas, M. and Basal, V. (2004). *Fuzzy controllers for tire slip control in anti-lock braking systems.* In Proc., IEEE Int. Conf. Fuzzy Systems 2004, 25 - 29 Jul 2004, vol. 3, pp. 1317-1322.

Rajamani, R. (2006). Vehicle Dynamics and Control, New York : Springer.

SAE (1992). Anti-lock Brake System Review, Technical Report J2246, Warrendale, PA: SAE.

Sahin, M. and Unlusoy, Y. S. (2010). *Design and simulation of an ABS for an integrated active safety system for road vehicles.* Int. J. Vehicle Design, 52(1-2-3-4), pp. 64-81.

Savaresi, S. M. and Tanelli, M. (2010). Active Braking Control Systems Design for Vehicles, London: Springer-Verlag.

Schinkel, M. and Hunt, K. (2002). *Anti-lock braking control using a sliding mode like approach.* In Proc., American Control Conf., 2002, vol. 3, pp. 2386-2391.

Shim, T., Chang, S. and Lee, S. (2008). *Investigation of sliding-surface design on the performance of sliding mode controller in antilock braking systems*. IEEE T. Veh. Technol., 57(2), pp. 747-759.

Slotine, J. J. E. and Li, W. (1991). Applied Nonlinear Control, London: Prentice-Hall.

Solyom, S. (2002). *Synthesis of a model-based tire slip controller*. Licentiate Thesis, Lund Institute of Technology.

Tan, H. S. and Chin, Y. K. (1991). *Vehicle traction control: Variable-structure control approach.* J. Dyn. Syst.-T. ASME, 113, pp. 223-230.

Tan, H. S. and Tomizuka, M. (1990). *An adaptive sliding mode vehicle traction controller design.* Proc. American Control Conf., 23 - 25 May 1990, San Diego, CA, USA, pp. 1856-1862.

Ünsal, C. and Kachroo, P. (1999). *Sliding mode measurement feedback control for antilock braking systems*. IEEE T. Contr. Syst. T., 7(2), pp. 271-281.

Wang, W., Li, I., Chen, M., Su, S. and Hsu, S. (2009). *Dynamic slip-ratio estimation and control of antilock braking systems using an observer-based direct adaptive fuzzy–neural controller*. IEEE T. Ind. Electron., 56(5), pp. 1746-1756.

Wellstead, P. E. and Pettit, N. B. O. L. (1997). *Analysis and redesign of an antilock brake system controller*. IEE P. Contr. Theor. Ap., 144(5), pp. 413-426.

Wu, M.-C. and Shih, M.-C. (2003). *Simulated and experimental study of hydraulic anti-lock braking system using sliding-mode PWM control.* Mechatronics, 13(4), pp. 331-351.

Yazicioglu, M. and Unlusoy, Y. S. (2008). *A fuzzy logic controlled anti-lock braking system (ABS) for improved braking performance and directional stability.* Int. J. Vehicle Design, 48(3-4), pp. 299-315.

Yi, J., Alvarez, L. and Horowitz, R. (2002). *Adaptive emergency braking control with underestimation of friction coefficient.* IEEE T. Contr. Syst. T., 10(3), pp. 381-392.

Yu, J. S. (1997). *A robust adaptive wheel-slip controller for antilock brake system.* In Proc., 36th IEEE Conf. Decision and Control, 10 - 12 Dec 1997, San Diego, CA, USA, vol. 3, pp. 2545-2546.

APPENDIX A

VEHICLE AND TIRE MODEL PARAMETERS

A.1. Vehicle Model

$m = 407.7\,kg \quad (F_{zo} / g)$

$J = 2\,kgm^2$

$r = 0.300\,m$

A.2. Magic Formula Tire Model

$C_x = p_{Cx1} \cdot \kappa_{Cx}$

$D_x = \mu_x \cdot F_z \cdot \zeta_1$

$\mu_x = \left(p_{Dx1} + p_{Dx2} df_z \right) \cdot \kappa^*_{\mu x}$

$E_x = \left(p_{Ex1} + p_{Ex2} df_z + p_{Ex3} df_z^2 \right) \cdot \left\{ 1 - p_{Ex4} \operatorname{sgn}\left(\lambda_x \right) \right\} \cdot \kappa_{Ex}$

$K_{x\lambda} = F_z \cdot \left(p_{Kx1} + p_{Kx2} df_z \right) \cdot \exp\left(p_{Kx3} df_z \right) \cdot \kappa_{Kx\lambda}$

$B_x = K_{x\lambda} / \left(C_x D_x + \varepsilon_x \right)$

$S_{Hx} = \left(p_{Hx1} + p_{Hx2} df_z \right) \cdot \kappa_{Hx}$

$S_{Vx} = F_z \cdot \left(p_{Vx1} + p_{Vx2} df_z \right) \cdot \left\{ \left| V_x \right| / \left(\varepsilon_{Vx} + \left| V_x \right| \right) \right\} \cdot \kappa_{Vx} \cdot \kappa^{'}_{\mu x} \cdot \zeta_1$

$\kappa^*_{\mu x} = \kappa_{\mu x} / \left(1 + \kappa_{\mu V} V_s / V_0 \right)$

$\kappa'_{\mu x} = 10\kappa^*_{\mu x} / \left\{1 + 9\kappa^*_{\mu x}\right\}$

$V_0 = 16.67\, m/s$ $F_{z0} = 4000\, N$

$p_{Kx1} = 21.510$ $p_{Kx2} = -0.163$ $p_{Kx3} = 0.245$

$p_{Cx1} = 1.685$ $p_{Dx1} = 1.210$ $p_{Dx2} = -0.037$

$p_{Ex1} = 0.344$ $p_{Ex2} = 0.095$ $p_{Ex3} = -0.020$

$p_{Ex4} = 0.0$

$p_{Hx1} = -0.002$ $p_{Hx2} = 0.002$ $p_{Vx1} = 0.0$

$p_{Vx2} = 0.0$

$\kappa_{Kx\lambda} = 1.000$ $\kappa_{Cx} = 1.000$ $\kappa_{\mu x} = 1.000$ (changes for varying road friction)

$\kappa_{\mu V} = 0.0$ $\kappa_{Ex} = 1.000$ $\kappa_{Hx} = 1.000$

$\kappa_{Vx} = 1.000$

$\varepsilon_x = 0.1$ $\varepsilon_{Vx} = 0.0$ $\zeta_1 = 1.000$